

Deep learning for table detection and structure recognition: A survey

Mahmoud Kasem^a, Abdelrahman Abdallah^a, Alexander Berendeyev^d,
Ebrahim Elkady^a, Mahmoud Abdalla^e, Mohamed Mahmoud^{a,f}, Mohamed
Hamada^b, Daniyar Nurseitov^{d,c}, Islam Taj-Eddin^a

^a*Information Technology Department, FCI, Assiut
University, Assiut, 71515, Assiut, Egypt*

^b*Department of Information System, International IT
University,, Almaty, 050000, Kazakhstan*

^c*KazMunayGas Engineering LLP, Nur-Sultan, 010000, Kazakhstan*

^d*Satbayev University, Almaty, 050013, Kazakhstan*

^e*Information Technology Institute(ITI), Alexandria, 5310002, Egypt*

^f*College of Electrical and Computer Engineering, Chungbuk National
University, Cheongju, 28644, South Korea*

Abstract

Tables are everywhere, from scientific journals, papers, websites, and newspapers all the way to items we buy at the supermarket. Detecting them is thus of utmost importance to automatically understanding the content of a document. The performance of table detection has substantially increased thanks to the rapid development of deep learning networks. The goals of this survey are to provide a profound comprehension of the major developments in the field of Table Detection, offer insight into the different methodologies, and provide a systematic taxonomy of the different approaches. Furthermore, we provide an analysis of both classic and new applications in the field. Lastly, the datasets and source code of the existing models are organized to provide the reader with a compass on this vast literature. Finally, we go over the architecture of utilizing various object detection and table structure recognition methods to create an effective and efficient system, as well as a set of development trends to keep up with state-of-the-art algorithms and future research. We have also set up a public GitHub repository where we will be updating the most recent publications, open data, and source code. The GitHub repository is available at <https://github.com/abdoelsayed2016/table-detection-structure-recognition>.

Keywords: Convolutional neural networks, deep learning, Document processing, table detection, table structure recognition.

1. Introduction

Textbooks, lists, formulae, graphs, tables, and other elements are common in documents. Most papers, in particular, contain several sorts of tables. Tables, as a significant part of papers, may convey more information in fewer words and allow readers to quickly explore, compare, and comprehend the content. Table detection and structure identification are crucial tasks in image analysis because they allow retrieving vital information from tables in a digital format. Because of the document's type and the variety of document layouts, detecting and extracting images or document tables is tough. Researchers have previously used heuristic techniques to recognize tables or to break pages into many parts for table extraction. Few studies have focused on table structure recognition in documents following table detection.

The layout and content analysis of documents are used to detect tables. Tables come in a number of layouts and formats. As a result, creating a general method for table detection and table structure recognition is quite difficult. Table detection is regarded as a difficult subject in scientific circles. A large number of studies have been conducted in this sector, although the majority of them have limitations. Existing commercial and open-source document analysis algorithms, such as Tesseract, are unable to fully detect table areas from document images. [1].

Machine learning and deep learning have been proven to be very effective in computer vision research. On computer vision tasks such as picture classification, object detection, object position estimation, learning, and so on, deep convolutional neural networks (types of feed-forward artificial neural systems) have outperformed alternative learning models. The effectiveness of Convolutional Neural Networks (CNNs) in object identification is based on their ability to learn substantial mid-level visual properties rather than the hand-crafted low-level representations that are often utilized in particular approaches to image categorization. The object is defined by its major characteristics, which include shape, size, color, texture, and other characteristics. To identify such an item, a picture must clearly reveal the object's presence and, moreover, its position [2].

Object detection may thus be described as a method of locating real-world items in photographs. Detection is closely connected to categorization

because it includes determining the existence and location of a certain item in an image. There are many items that may be identified in a picture, including automobiles, buildings, tables, human faces, and so on. Deep learning approaches, such as deep neural networks, region-based convolutional neural networks, and deeply convolutional neural networks, can improve object identification precision, and efficacy.

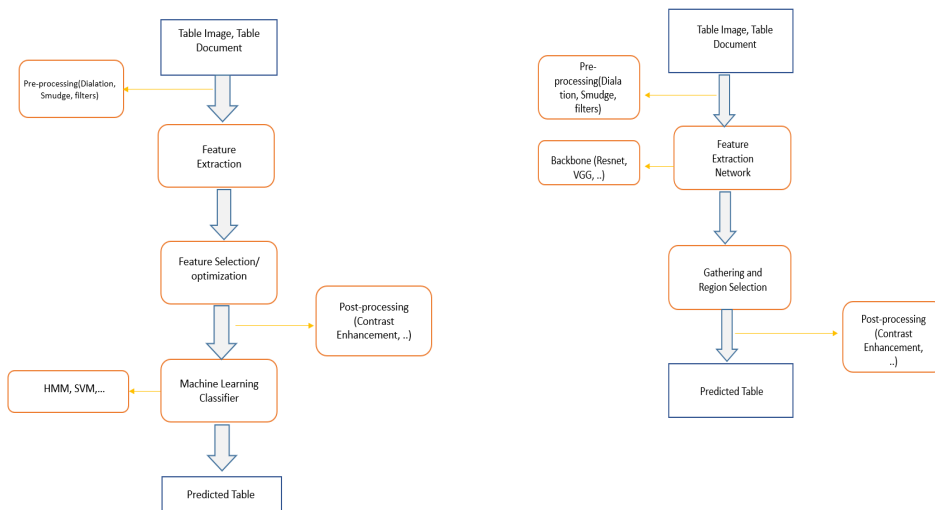
In recent years, a variety of remarkable and creative strategies have been used to improve deep learning model detection accuracy and solve complex challenges encountered during the training and testing process of deep learning object recognition models. Modification of the activation function of deep CNNs [3], Transfer learning [4, 5], cancer diagnosis, detection [6, 7, 8], and classification[9], and medical question answers[10, 11], as well as software engineering applications such as optimizing the time and schedule of software projects[12, 13], Intrusion Detection in IoT [14, 15] and handwritten recognition for various languages[16, 17, 18, 19]., and inventive ways in the combined selection of the activation function and the optimization system for the proposed deep learning model are among these unique strategies. Among the various variables and initiatives that have contributed to the rapid advancement of table detection algorithms, the development of deep convolutional neural networks and GPU computational capacity should be credited. Deep learning models are now widely used in many aspects of computer vision, including general table detection[20, 21, 22, 23, 24]. Table structures, on the other hand, receive far less attention, and the table structure is typically characterized by the rows and columns of a table [25, 26, 27].

Figure 1 shows a basic pipeline comparison of deep learning techniques and conventional approaches for the task of understanding tables. Traditional table recognition techniques either can't handle varied datasets well enough or need extra metadata from PDF files. Extensive pre- and post-processing were also used in the majority of early approaches to improve the effectiveness of conventional table recognition systems. However, deep learning algorithms retrieve features using neural networks, primarily convolutional neural networks [21], instead of manually created features. Object detection or segmentation networks then try to differentiate the tabular portion that is further broken down and recognized in a document image.

This survey examines deep learning-based table detection and classification architectures in depth. While current evaluations are comprehensive [28, 29], the majority of them do not address recent advancements in the field.

The following are the paper’s main contributions:

1. We provide a brief history of Table Datasets and the differences between them.
2. The paper examines important table detection methods, as well as the evolution of these methods over time.
3. We give a thorough analysis of table structure recognition in-depth.
4. We provide Table Classification methods and compare these methods. There was no study that provided a broad summary of these issues that we could identify.
5. Experiments Result on some datasets of Table detection



(a) Traditional Table Detection approaches (b) Deep Learning approaches for Table Detection

Figure 1: Table analysis pipeline comparison of conventional and deep learning methods. While convolutional networks are used in deep learning techniques, classical approaches primarily perform feature extraction through image processing techniques. Deep learning methods for interpreting tables are more generalizable and independent of data than conventional approaches.

1.1. Comparison with Previous Reviews

For many years, the issue with table analysis has been widely acknowledged. Figure 2 shows the upward trend in publications during the previous

eight years, this analysis values were derived from Scopus. There have been notable table detection and table classification surveys published. There are outstanding studies on the subject of table detection in these surveys [28, 29]. There have been few recent surveys that specifically address the subject of table detection and classification. B. Coüasnon [30] released another review on table recognition and forms. The review gives a quick rundown of the most recent techniques at the time, S. Khusro [31] released the most recent review on the identification and extraction of tables in PDF documents the following year, according to our knowledge. Deep learning enables computational models to learn fantastically complex, subtle, and abstract representations, resulting in significant advancements in a wide range of problems such as visual recognition, object detection, speech recognition, natural language processing, and medical image analysis. In contrast, despite the fact that various deep learning-based algorithms for table identification have been presented, we are unaware of any recent thorough survey. For further advancement in table detection, a detailed review and explanation of prior work are required, especially for researchers new to the topic.

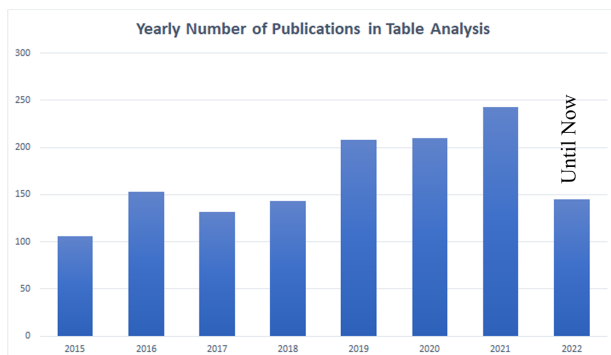


Figure 2: shows an illustration of an expanding trend in the area of table analysis. This information was gathered by looking through the annual reports on table detection and table identification from the years 2015 to 2022, this analysis values were derived from Scopus.

1.2. Scope

The quantity of studies on deep learning-based table detection is staggering. They are so numerous that any complete examination of the state of the art would be beyond the scope of any acceptable length paper. As a result, selection criteria must be established, and we have narrowed our attention to the best journal and conference articles.

The main goal of this paper is to provide a comprehensive survey of deep learning-based table detection and classification techniques, as well as some taxonomy, a high-level perspective, and organization, based on popular datasets, evaluation metrics, context modeling, and detection proposal methods. Our goal is for our classification to make it easier for readers to comprehend the similarities and differences across a wide range of tactics. The suggested taxonomy provides a framework for researchers to comprehend existing research and highlight open research problems for the future.

2. Major Challenges

2.1. Object detection Challenges

Developing a general-purpose algorithm that fulfills two competing criteria of high quality/accuracy and great efficiency is ideal for object detection. High-quality detection must accurately localize and recognize objects in images or video frames, allowing for distinction of a wide range of object categories in the real world and localization and recognition of object instances from the same category, despite intra-class appearance variations, for high robustness. High efficiency necessitates that the full detection process is completed in real-time while maintaining reasonable memory and storage requirements.

2.2. Table detection Challenges

Although a trained segmentation model can accurately locate tables, conventional machine learning techniques have flaws in the structural identification of tables. A major issue is a large number of things in such a little space. As a result, the network misses out on critical visual cues that may aid in the detection and recognition of tables [20]. As physical rules are available, intersections of horizontal and vertical lines are computed to recognize table formations. The Hough transform is a prominent approach in computer vision that aids in the detection of lines in document scans [32]. Length, rotation, and average darkness of a line are utilized to filter out false positives

and determine if the line is, in fact, a table line [33]. The intersections of the remaining horizontal and vertical lines are computed after the Hough lines have been filtered. Table cells are created based on the crossings.

3. A Quick Overview of Deep Learning

From image classification and video processing to speech recognition and natural language understanding, deep learning has transformed a wide range of machine learning activities. Given the incredible rate of change[34], there is a plethora of current survey studies on deep learning [35, 36, 37, 38, 39, 40, 41, 42, 43, 44, 45] , medical image analysis applications [38], natural language processing [42], and speech recognition systems [44].

Convolutional neural networks (CNNs), the most common deep learning model, can use the fundamental properties of actual signals: translation invariance, local connection, and compositional hierarchies. A typical CNN comprises a hierarchical structure and numerous layers for learning data representations at different levels of abstraction [36]. We start with a convolution

$$x^{l-1} * w^l \tag{1}$$

between a feature map from the previous layer l-1 and an input feature map x^{l-1} , convolved using a 2D convolutional kernel (or filter or weights) w^l . This convolution is seen as a series of layers that have been subjected to a nonlinear process σ , such that

$$x_j^l = \sigma \left(\sum_{i=1}^{N^{l-1}} x_i^{l-1} * w_{i,j}^l + b_j^l \right) \tag{2}$$

with a bias term b_j^l and a convolution between the N^{l-1} input feature maps x_i^{l-1} and the matching kernel $w_{i,j}^l$. For each element, the element-wise nonlinear function $\sigma(\cdot)$ is commonly a rectified linear unit (ReLU) for each element,

$$\sigma(x) = \max\{x, 0\} \tag{3}$$

Finally, pooling is the process of downsampling and upsampling feature maps. Deep convolution neural networks(DCNNs) are CNNs with a large number of layers, often known as "deep" networks . A CNN's most basic

layers consist of a series of feature maps, each of which operates as a neuron. A set of weights $w_{i,j}$ connects each neuron in a convolutional layer to feature maps from the preceding layer (essentially a set of 2D filters). Whereas convolutional and pooling layers make up the early CNN layers, the subsequent layers are usually completely connected. The input picture is repeatedly convolved from earlier to later layers, and the receptive field or region of support grows with each layer. In general, the first CNN layers extract low-level characteristics (such as edges), whereas subsequent layers extract more generic features of increasing complexity. [35, 46, 47, 36].

DCNNs have a hierarchical structure that allows them to learn data representations at numerous levels of abstraction, the ability to learn highly complicated functions, and the ability to learn feature representations directly and automatically from data with minimum domain expertise. The availability of huge size labeled datasets and GPUs with extremely high computational capabilities is what has made DCNNs so successful.

Despite the enormous achievements, there are still acknowledged flaws. There is a critical need for labeled training data as well as expensive computational resources, and selecting proper learning parameters and network designs still requires substantial expertise and experience. Trained networks are difficult to comprehend, lack resistance to degradations and many DCNNs have been proven to be vulnerable to assaults [37], all of which restrict their applicability in real-world applications.

4. Datasets and Evaluation Metrics

4.1. Datasets

This section will describe datasets that are available and have been most commonly used for table detection, table structure recognition, and classification tasks.

4.1.1. ICDAR 2013

ICDAR2013 dataset[48] referred to in served as the competition’s official practice dataset. Rather than focusing on a specific subset of documents, authors have always intended to evaluate systems as broadly as possible, and this dataset, as well as the actual competition dataset, were generated by systematically collecting PDFs from a Google search in order to make the selection as objective as possible. they are limited to two governmental

sources with the additional search terms `site:europa.eu` and `site:*.gov` in order to obtain documents whose publications are known to be in the public domain. The ICDAR2013 dataset contains 150 tables, 75 of which are in 27 EU excerpts and 75 of which are in 40 US Government excerpts. Table regions are rectangular areas of a page whose coordinates define them. Multiple regions can be included in the same table because a table can span multiple pages. Table detection or location and table structure recognition are the two sub-tasks of ICDAR2013. The task of table structure recognition compares methods for determining table cell structure given precise location information. Figure 3 presents a few examples from this dataset.

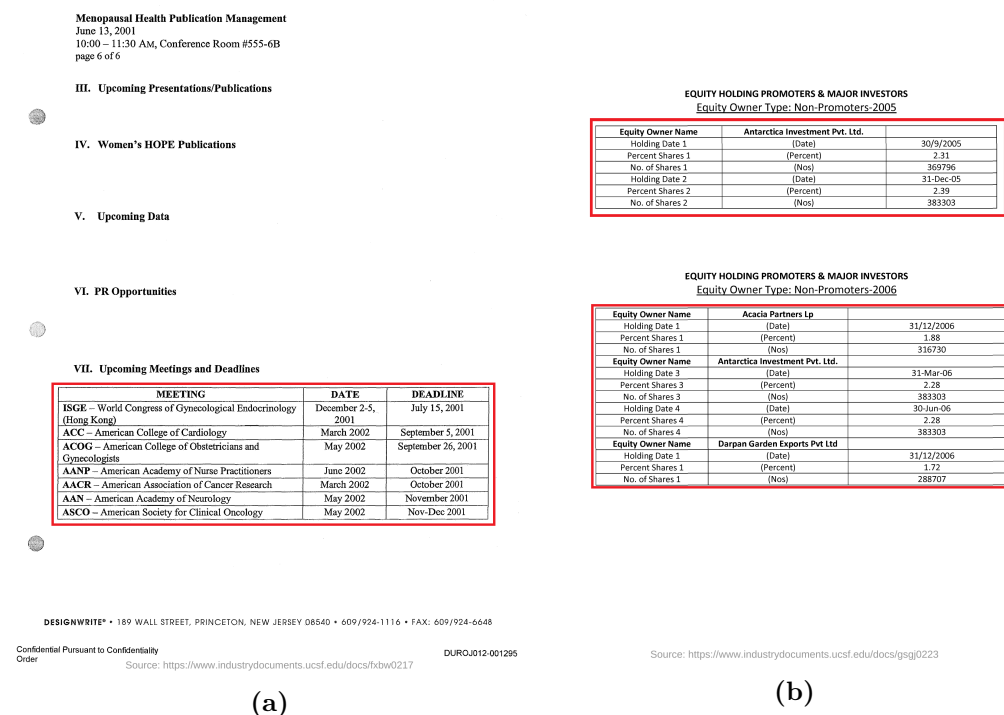
4.1.2. ICDAR 2017 POD

Dataset [49] was published for the ICDAR2017 Page Object Detection (POD) competition. This dataset is frequently used to test different methods of table detection. Compared to the ICDAR2013 table dataset, this dataset is significantly larger. There are 2417 total images in it, including figures, tables, and formulae. The dataset is commonly split into 1600 photos which have 731 tabular areas for training, and the remaining 817 images which have 350 tabular regions for testing. Figure 4 illustrates two examples of this dataset.

4.1.3. ICDAR2019

ICDAR2019 [50] proposed a dataset for table detection (TRACK A) and table recognition (TRACK B). The dataset is divided into two types, historical and modern datasets. It contains 1600 images for training and 839 images for testing. The historical type contains 1200 images in tracks A and B for training and 499 images for testing. The modern type contains 600 images in tracks A and B for training and 340 images for testing. Document images containing one or more tables are provided for TRACK A. TRACK B has two sub-tracks: the first (B.1) provides the table region, and only the table structure recognition is required. The second sub-track (B.2) contains no prior knowledge. That is, both table region detection and table structure recognition must be performed. For the annotation of the dataset, a similar notation was derived from the ICDAR 2013 [48] Table Competition format, and the structures were stored in a single XML file. Each table element corresponds to a table with a single `Coords` element with a `points` attribute indicating the coordinates of the bounding polygon with `N` vertices. Each table element contains a list of cell elements as well. The attributes `start-row`,

start-col, end-row, and end-col denote the position of each cell element in the table. The cell element's Coords denote the coordinates of the bounding polygon of this cell box, and the content is the text within this cell. Figure 5 presents a few examples from this dataset.



(a)

(b)

Figure 3: Examples of images in ICDAR 2013

4.1.4. TabStructDB

TabStructDB is a different publicly available image-based table structure recognition dataset that was promoted by SA Siddiqui [51]. The well-known ICDAR 2017 page object detection dataset, which contains pictures annotated with structural details, was used to curate this dataset. Figure 6 illustrates two examples of this dataset.

4.1.5. TABLE2LATEX-450K

TABLE2LATEX-450K [52] is another sizable dataset that was released at the most recent ICDAR conference. The dataset includes 450,000 annotated

VII GTC Code for Prevention of Insider Trading

In accordance with the Securities and Exchange Board of India (Prohibition of Insider Trading) Regulations, 1992, the Board of Directors of the Company formulated the GTC Code of Conduct for Prevention of Insider Trading in the shares and securities of the Company by its employees. The GTC Code, inter alia, prohibits purchase/sale of shares by employees, while in possession of unpublished price sensitive information in relation to the Company. Shri Kamal K. Gupta, Vice President (Corporate Affairs) & Secretary has been appointed as the Compliance Officer by the Board of Directors to implement the provisions of the aforesaid Insider Trading Regulations.

III General Shareholders Information

(i) 49th Annual General Meeting

The Annual General Meeting for the year ended 31st March, 2005 is scheduled to be held on Thursday, the 15th of September, 2005 at 3.00 pm., at Shri Bhadras Maganlal Sabhagha, U-1, Juhu Development Scheme, Vile Parle (West), Mumbai - 400056.

(ii) Financial Calendar

Calendar of events for the Financial Year 2005-2006 is as under:

Unaudited First Quarter Results	By end of July, 2005
Audited Annual Results for Previous Year ended 31 st March, 2005.	By end of June, 2005
Unaudited Second Quarter Results	By end of October, 2005
Unaudited Third Quarter Results	By end of January, 2006
Unaudited Fourth Quarter Results	By end of April, 2006

(iii) Date of Book Closure

Friday, the 9th day of September, 2005 to Thursday, the 15th day of September, 2005 (both days inclusive).

(iv) Listing on Stock Exchanges and Stock Code

Name of the Stock Exchange	Stock Code No.
National Stock Exchange of India Ltd., Exchange Plaza, 5 th Floor, Plot No. C/1, 'G' Block, Bandra - Kurla Complex, Mumbai - 400 051.	5251
The Stock Exchange, Mumbai Phoenix Jejeebhoy Towers, Dalal Street, Mumbai - 400 001.	151
The Calcutta Stock Exchange Association Ltd. 7, Lyons Range, Calcutta - 700 001.	-

The Company had vide special resolution passed at the Annual General Meeting held on 24th September, 2003 approved the delisting of the equity shares of the Company from eight stock exchanges where it was previously listed except National Stock Exchange of India Ltd. And Stock Exchange, Mumbai. Applications had been forwarded to the concerned exchanges to delist the shares of the Company, of which approval has been accorded to delisting from the following stock exchanges:

Sr. No.	Name of Stock Exchange	Effective Date of Delisting
1.	The Veddara Stock Exchange Ltd.	0 th February, 2005

Application for delisting is pending approval from The Calcutta Stock Exchange Association Ltd. The listing fees for the year 2005-2006 has been paid to National Stock Exchange of India Ltd. And Stock Exchange, Mumbai in time.

Source: <https://www.industrydocuments.ucsf.edu/docs/gsqj0223>

TABLE 6.05

INDICATIONS FOR IMPLANTATION

	WOVEN	KNITTED	VELOURS	TOTAL
Aneurism	1 *	7 *	6 *	14
Claudication		21 *	7 *	28
Coarctation of the aorta	1			1
Congenital malformation			1	1
TOTAL	2	28	14	44

* Includes 5 ruptured aneurisms cases

The following anecdotal observations are worthy of mention in connection with the autopsy data. Neovascularization with endothelial-like cell development was noted in only four cases. In all instances it was confined to small patches on or near the anastomosis or on isolated areas not far from the anastomotic site: an aorto-femoral Weavennit after 17 months of implantation in a elective patient (48 years-old, abdominal aorta aneurism, iliac stenosis), a well healed Weavennit bifurcation implanted for 50 months in a 55 years-old patient treated for claudication, a Knitted de Bakay implanted for 98 months after resection of an abdominal aneurism in a 64 years-old patient and a Knitted de Bakay implanted for 84 months in two femoro-popliteal positions to bypass bilateral blockage in a 58 years-old candidate. In summary, there are relatively few points in common for all these patients other than the observation that they were somewhat younger and free of additional degenerative disease such as diabetes. Three Microvel prostheses (figure 6.06) implanted by the same surgeon and collected after two months, showed radically different healing characteristics; the first, B16, was the best in spite of the fact that it originated from a high risk patient (75 years-old, emergency surgery for a ruptured aneurism, post-operative kidney failure). All traces of healing were absent from a second prosthesis, B25, which originated from an elective patient (71 years old, diabetic). This same patient had an uneventful post-operative recovery. The third device, B58, was also from an elective patient (59 years old, aneurism of the aorta). This device exhibited only a thin coat of fibrin with a smooth surface but without densification or organ-

65

Source: <https://www.industrydocuments.ucsf.edu/docs/gsqj0226>

(a)

(b)

Figure 4: Examples of images in ICDAR 2017

tables and the associated pictures. This enormous dataset was created by crawling through all of the LaTeX source documents and ArXiv publications from 1991 to 2016. The high-quality labeled dataset is obtained via source code extraction and further refining. Figure 7 presents a few examples from this dataset.

4.1.6. RVL-CDIP (SUBSET)

A well-known dataset in the world of document analysis is the RVL-CDIP (Ryerson Vision Lab Complex Document Information Processing) [53]. 400,000 photos are included, evenly spread over 16 classifications. For the purpose of detecting tables, P Riba [54] makes subset dataset by annotating the 518 invoices in the RVL-CDIP dataset. The dataset has been made available to the general public. For testing table identification methods especially created for invoice document pictures, this subset of the real RVL-CDIP dataset [53] is a significant contribution. Figure 8 presents a few examples

EQUITY HOLDING PROMOTERS & MAJOR INVESTORS
Equity Owner Type: Non-Promoters-2005

Equity Owner Name	Antarctica Investment Pvt. Ltd.	
Holding Date 1	(Date)	30/9/2005
Percent Shares 1	(Percent)	2.31
No. of Shares 1	(Nos)	369796
Holding Date 2	(Date)	31-Dec-05
Percent Shares 2	(Percent)	2.39
No. of Shares 2	(Nos)	383303

EQUITY HOLDING PROMOTERS & MAJOR INVESTORS
Equity Owner Type: Non-Promoters-2006

Equity Owner Name	Acacia Partners Lp	
Holding Date 1	(Date)	31/12/2006
Percent Shares 1	(Percent)	1.88
No. of Shares 1	(Nos)	316730
Equity Owner Name	Antarctica Investment Pvt. Ltd.	
Holding Date 3	(Date)	31-Mar-06
Percent Shares 3	(Percent)	2.28
No. of Shares 3	(Nos)	383303
Holding Date 4	(Date)	30-Jun-06
Percent Shares 4	(Percent)	2.28
No. of Shares 4	(Nos)	383303
Equity Owner Name	Darpan Garden Exports Pvt Ltd	
Holding Date 1	(Date)	31/12/2006
Percent Shares 1	(Percent)	1.72
No. of Shares 1	(Nos)	288707

Source: <https://www.industrydocuments.ucsf.edu/docs/hsgj0223>

(a)

TABLE 4.1
ETHIOPIA 1998: PERCENTAGE OF ETHIOPIANS WITH ONE OR MORE
BRUACES, MISSING, OR FILLED PREGNANT TOOTH

Age Group	SOUTHERN ETHIOPIA (South of Addis Ababa)		CENTRAL ETHIOPIA (North of Addis Ababa)		NORTHERN ETHIOPIA (Tigray)	
	Number Examined	Percent DMP	Number Examined	Percent DMP	Number Examined	Percent DMP
5-9	20	10.0	10	0.0	32	12.5
10-14	202	7.4	54	1.9	54	35.2
15-19	79	11.4	50	8.0	12	16.7
20-29	59	22.0	76	10.5	28	35.7
30-39	28	40.7	75	29.3	21	23.8
40-49	27	33.3	47	34.0	11	54.5
50 +	21	19.0	50	48.0	27	55.6
Percent Caries-free	85.5		79.2		67.0	

TABLE 4.2
ETHIOPIA 1998: ANALYSIS OF WATER SAMPLES

	CALCIUM P.p.m.	MILQIUM P.p.m.	IRON P.p.m.
Alemayn	89	0.17	0.13
Keren	28	0.91	0.02
Gafarsa River	1.2	0.14	0.22
Harar	41	0.21	0.03
Arkiko	362	0.57	0.07
Gondar	15	0.14	0.48

(b)

Figure 5: Examples of images in ICDAR 2019

name	# blocks	# variables		# generated function terms
		# global	avg./block	
Driver "A"	3903	1	1.0	2840
Driver "B"	4022	2	2.3	2951
Driver "C"	3925	2	2.0	2860
Driver "D"	4487	2	2.0	3124
Driver "E"	3933	4	4.0	2868
Driver "F"	4519	6	9.2	37365
Driver "G"	4521	5	13.4	4395
Driver "H"	6760	18	39.5	14612
Driver "I"	5429	3	4.3	9744
Driver "J"	8693	1	1.0	7250
Driver "K"	4569	7	20.7	29984

(a)

region (x,y,x mm)	size (n)	Zmax	P(n _{max} > n)	P(Z _{max} > Z)
-54 -50 8	570	4.59	0.076	0.012
54 -48 4	697	4.42	0.041	0.024
0 -82 40	385	4.10	0.200	0.084
-44 46 -4	540	3.67	0.089	0.350

(b)

Figure 6: Examples of images in TabStructDB

from this dataset.

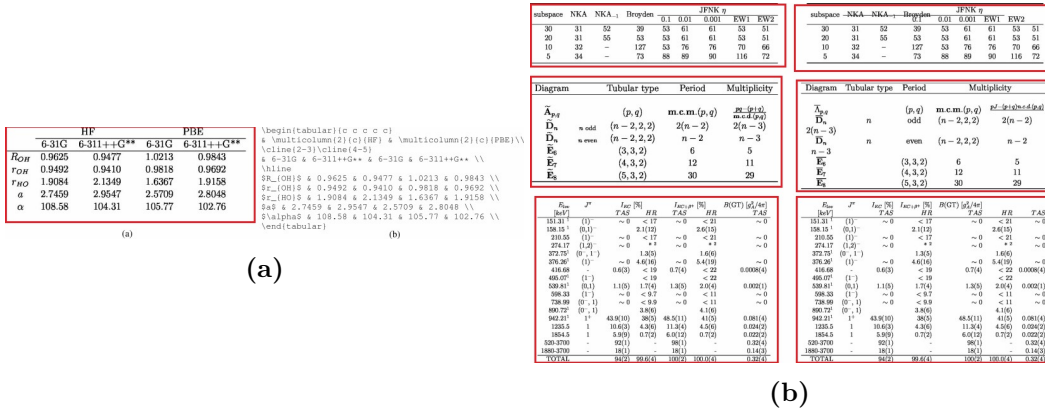


Figure 7: Examples of images in TABLE2LATEX-450K

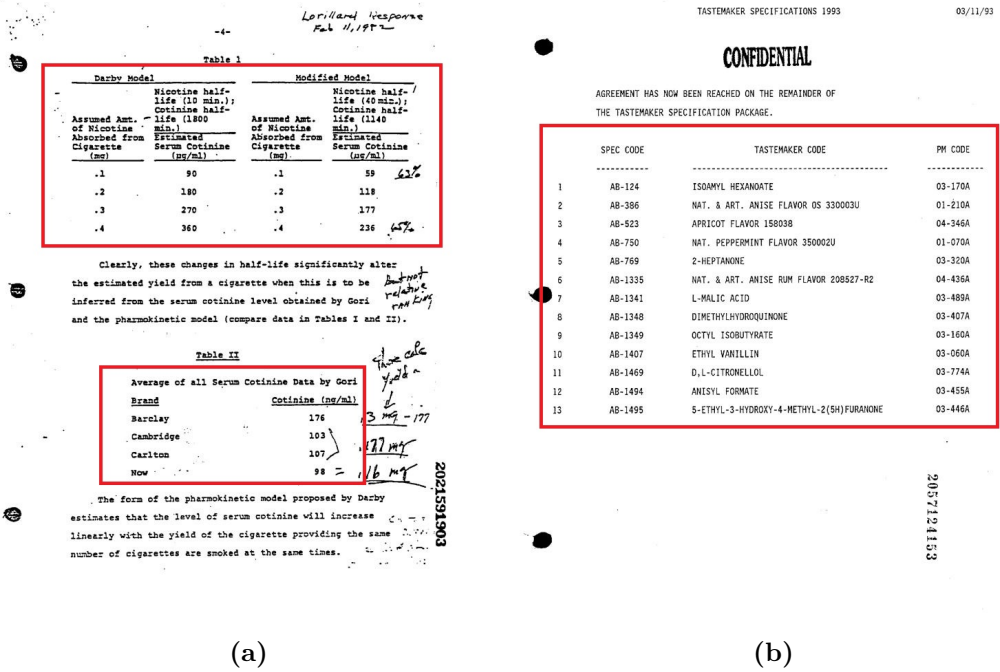
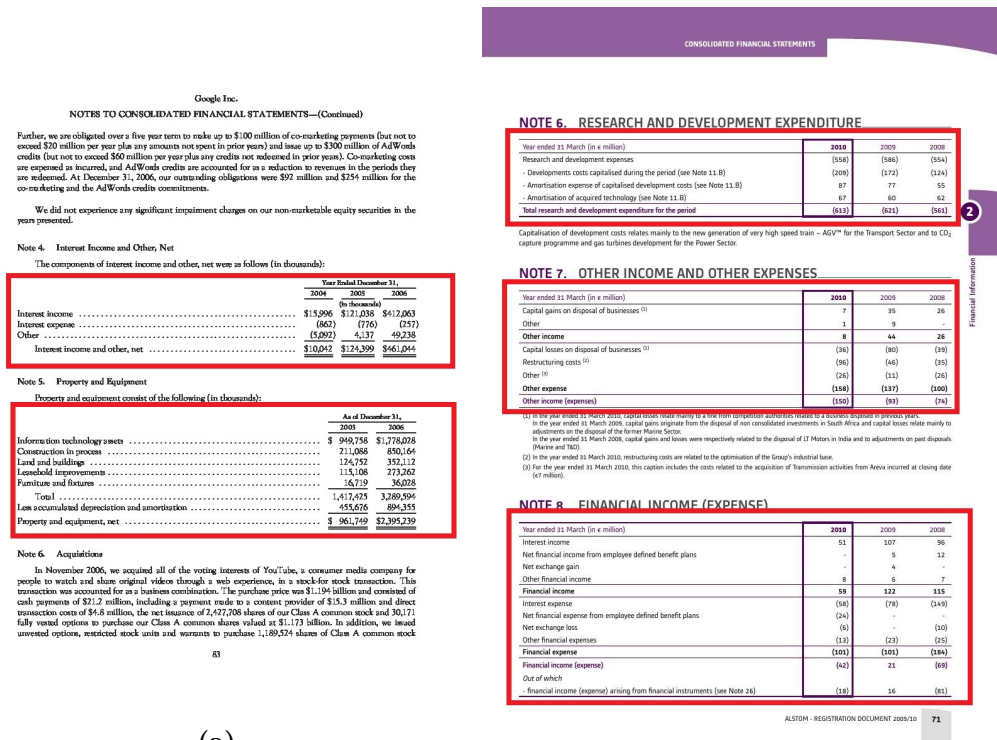


Figure 8: Examples of images in RVL-CDIP (SUBSET)

4.1.7. IIT-AR-13K

IIT-AR-13K is a brand-new dataset that is introduced by A Mondal [55]. The yearly reports that were publicly available and written in English and

other languages were collected to create this dataset. The biggest manually annotated dataset for the problem of graphical page object recognition, according to the authors, has been released. Annotations for figures, natural imagery, logos, and signatures are included in the dataset in addition to the tables. For numerous tasks of page object detection, the authors have included the train, validation, and test splits. In order to train for table detection, 11,000 samples are employed, while 2000 and 3000 samples are allotted for validation and testing, respectively. Figure 9 illustrates two examples of this dataset.



(a)

(b)

Figure 9: Examples of images in IIIT-AR-13K

4.1.8. CamCap

CamCap is a collection of camera-captured photos suggested by W Seo [56]. Only 85 photos are present (38 tables on curved surfaces having 1295 cells and 47 tables on planar surfaces consisting of 1162 cells). For the sake

of detecting tables and identifying their structures, the suggested dataset is accessible to the general public. This dataset is a significant addition to evaluating the reliability of table identification techniques on camera-captured document pictures. Figure 10 illustrates two examples of this dataset.

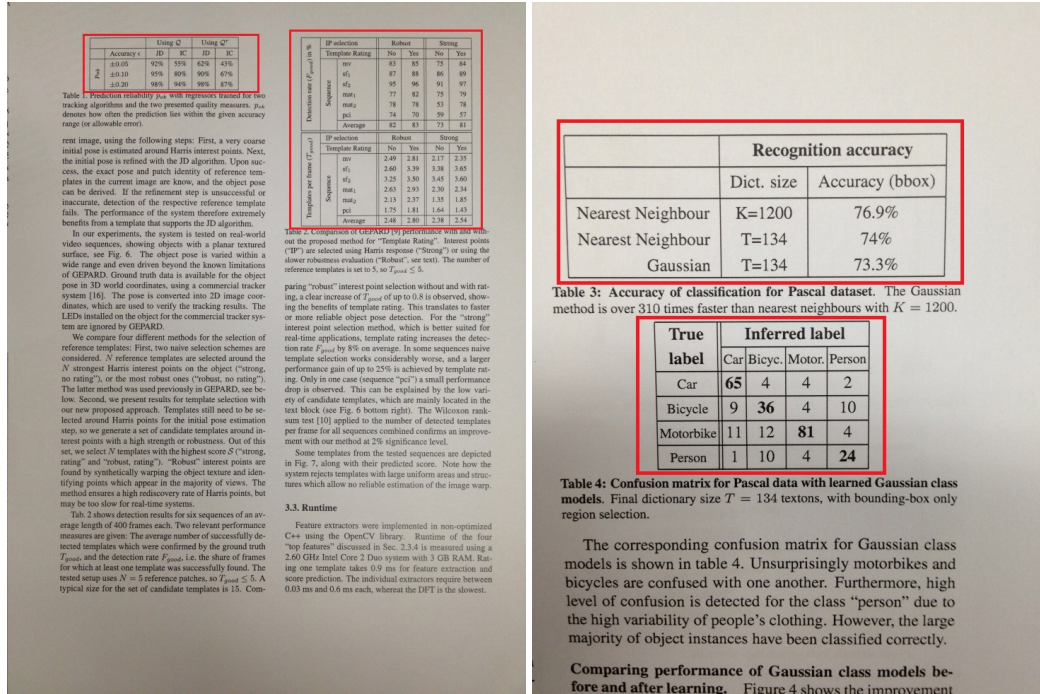


Figure 10: Examples of images in CamCap

4.1.9. UNLV Table

The UNLV Table dataset[57] includes 2889 pages of scanned document images gathered from various sources (magazines, newspapers, business letters, annual reports, etc). Scanned images are available in bitonal, grayscale, and fax formats, with resolutions ranging from 200 to 300 DPI. There is ground truth data in addition to the original dataset, which contains manually marked zones; zone types are provided in text format. Figure 11 illustrates two examples of this dataset.

4.1.10. UW-3 Table

The UW-3 Table dataset [58] contains 1600 skew-corrected English document images with manually edited entity bounding box ground-truth. Page frames, text and non-text zones, text lines, and words are all surrounded by these bounding boxes. Each zone's type (text, math, table, half-tone, etc.) is also indicated. There are approximately 120 document images with at least one marked table zone. The UNLV and UW-3 Table dataset taught a user how to use the T-Truth tool and asked him to prepare ground truth for the target images in the above dataset. Each image's ground truth is stored in an XML. Another expert manually validated the ground truths using the T-Truth tool's preview edit mode, and incorrect ground truths were corrected. These iterations were repeated several times to ensure that the ground truth was correct. authors discovered that the majority of errors occur when labeling column spanning cells where the column boundaries coincide with the word boundaries. Problems can also arise when there are multiple interpretations of a table structure, as described by Nagy[59], and domain knowledge is required to correctly label the table structure. Figure 12 illustrates two examples of this dataset.

4.1.50

TABLE 4.1.26. Capital Cost Estimate for the Waste Calculation Facility

Cost Element	Man-hours - 1000s		Costs, 1000s of 1976 Dollars	
	Manpower	Mechanical	MATERIAL	LABOR
Major equipment	40	3,400	500	4,100
Building and structures	900	3,000	6,100	9,100
Bulk materials	470	6,400	8,000	16,400
Site improvements	10	100	100	200
Subtotal of direct site construction costs	1,220	15,100	14,700	29,000
Indirect site construction costs	320	240	5,400	7,100
Total field cost	1,540	15,340	20,100	36,100
Architect-engineer services	200	1,400	20,000	21,800
Subtotal				57,900
Owner's cost				15,000
Total facility cost				72,900
Estimated accuracy range				±30%

TABLE 4.1.27. Operating Cost Estimate for the Waste Calculation Facility

Cost Element	Annual Costs, \$1000s
Direct labor	840
Process materials	920
Utilities	100
Maintenance materials	300
Overhead	680
Miscellaneous	650
Total	3590 ±25%

Levelized Unit Cost. The levelized unit cost, including the levelized capital and operating segments, is shown in Table 4.1.28. The unit cost calculation assumes private ownership of the facilities and a 15-year economic life.

5.6.1B

TABLE 5.6.7. Krypton Gas Cylinder Storage Capital Cost Estimate, Phase II

Cost Element	Man-hours, 1000s		Costs, 1000s of 1976 Dollars	
	Manpower	Mechanical	MATERIAL	LABOR
Major equipment	5	100	100	200
Buildings and structures	760	12,400	9,100	21,600
Bulk materials	60	800	700	1,500
Site improvements	5	100	100	200
Subtotal of direct site construction costs	830	13,300	10,000	23,300
Indirect site construction costs	220	170	3,200	4,800
Total field cost	1,050	13,470	13,200	28,100
Architect-engineer services				4,400
Subtotal				32,500
Owner's cost				12,500
Total facility cost				45,000
Estimated accuracy range				±20%

Note: Costs for Phase III are the same as for Phase II.

The estimates in the tables cover all capital costs resulting from constructing the reference facility as an independently operated facility located a short distance from, but within the property limits of, the FRP. The reference facility is provided with its own machinery and switch gear room, maintenance area, and personnel areas, including change and shower room, restrooms and offices. Electrical power and water are supplied from the FRP. No portion of the general FRP costs for services, such as laboratories, warehousing, shops, and administration buildings, is allocated to the krypton storage facility.

The total capital cost includes the cost of the transfer cask and all plant-related costs incurred from the start of engineering to the initiation of operation with the exception of working capital.

Operating Costs. The operating costs for the krypton gas cylinder storage facility are shown in Table 5.6.8. Direct labor costs are based on manpower estimates given in Table 5.6.2. Utility costs are derived from requirements described in Section 5.6.1.5. Process materials costs are minimal (cost of storage cylinders are allocated to DOG treatment, Section 4.9.3). Annual maintenance material costs are estimated at 2% of major equipment costs. Overhead and miscellaneous costs are estimated using the standard method described in Section 3.8. The estimates for the miscellaneous items include all unidentified operating costs. The cost of taxes, insurance, and interest are included in the capital charge segment of the levelized unit cost.

(a)

(b)

Figure 11: Examples of images in UNLV

Method	Number	Technical procedure Title	Date
Rock bolt installation	TP-37	Procedure for installation of rock bolts	TBD
Evaluation of blasted rock	TP-38	Procedure for blasted rock sorting and size evaluation	TBD
Excavation activities	TP-41	Procedure for drilling and blasting	TBD
	TP-42	Procedure for loading and blasting	TBD

TBD = to be determined.
 MPBX = multiple-point borehole extensometers.

8.3.1.15.1.6 Study: In situ thermochemical properties

The objective of this study is to obtain data on in situ thermal and thermochemical properties for units T8w1 and T8w2. Properties to be obtained include heat capacity, thermal conductivity, and thermal expansion. Deformation modulus, strain ratio, and radon emanation rates also will be determined during some of the testing activities. In addition, the effects of heating on in situ water content, deformation modulus, changes in thermally induced stress, radon emanation, and the deformation response of the rock around a heated room will be observed. Some of the data will be used for validation of computer codes used in heat transfer and thermo-mechanical calculations. Additional heater experiments will be conducted to characterize the waste container environment, as discussed in Section 8.3.4.2.4.

Interpretation of the data to be obtained from the activities for this study will utilize information gathered for Study 8.3.1.4.2.2 (characterization of the structural features within the site area).

8.3.1.15.1.6.1 Activity: Heater experiment in unit T8w1

Objectives

The objectives of this activity are to estimate the in situ thermo-mechanical properties of lithophys-rich tuff (unit T8w1) and to observe the thermal and mechanical response of this tuff unit to elevated temperatures.

8.3.1.15-49

(a)

Finding Direction Cosines for a Given Plane

347

S 50° E. Coordinate axes will be taken as follows: x is horizontal to the east; y is horizontal north; and z is upward.
 The bearing of the upward normal to the plane is the same as the bearing of its dip, and it runs at a vertical angle complement to the amount of dip. To apply Equations A1.16 to calculate the stresses across the given plane, given the local state of stress, we describe each of the axes x' , y' , z' by a horizontal angle (θ) and a vertical angle (ϕ) as shown in Figure A1.13; θ is the counterclockwise angle from x to the horizontal projection of the axis in question while ϕ is the vertical angle between the axis and its horizontal projection. The line Ox' is in the direction of the upward normal. It proves convenient to take y' positive when directed up the steepest slope of the plane, that is, opposite to the dip vector, and z' along the strike, as shown in Figure A1.9. For the indicated bedding plane then, the bearings and rise angles of the three axes are (Figure A1.12):

Line	Compass Bearing	(θ)	Rise Angle (ϕ) (Positive if Above-Horizontal)
x'	S 50° E	-40°	55°
y'	N 50° W	140°	35°
z'	S 40° W	-130°	0

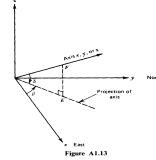


Figure A1.13

(b)

Figure 12: Examples of images in UW3

4.1.11. Marmot

The Marmot dataset[60] is considered the first large dataset in table detection. it contains 2000 PDF pages with ground truth data. This labeling task was completed by 15 people. To reduce subjectivity, a unified labeling standard was established, and each ground-truth file is double-checked. The dataset's size is still growing. The e-document pages in the dataset have a wide range of language types, page layouts, and table styles. First, it is made up of roughly equal parts Chinese and English pages. The Chinese pages were chosen from over 120 e-Books with diverse subject areas from Founder Apabi's digital library, with no more than 15 pages chosen from each book. The English pages were retrieved from the web. Over 1500 conference and journal papers from 1970 to 2011 were crawled, covering a wide range of topics. The Chinese e-Book pages are mostly one column, whereas the English pages are printed in both one and two columns. This dataset includes a wide range of table types, from ruled tables to partially and non-ruled tables, horizontal tables to vertical tables, inside-column tables to span-column tables, and so on. A few samples from this dataset are shown in Figure 13.

Table 2: Characteristics of VC Investments

Table 2 reports the characteristics of VC investments based on discrete responses by firms. Panel A refers to investment stage and reports the proportion of funds investing in different investment stages: "early" refers to seed and start-up, "middle" to expansion and growth, and "late" to later stages. Panel B refers to the sectors of investment using five groups of industries: life sciences, IT and software, electrical and semi-conductors, manufacturing and chemicals, and other industries (further discussion of the calculation used to derive these results is in the text). Panel C records the percentage of funds investing in one, two, three, or four or more industries. Panel D records the regional, national or international nature of investments by funds. It reports the percentage of funds investing in a region within a country, in several regions within a country, within a single continent, or in two or more continents (or in the case of Japan if more than 50 percent is invested abroad). * and ** denote mean values which are statistically different from those of the UK at the 10 and 5 percent levels, respectively.

Panel A: VC Investments by Stage

	Funds	Early (1)	Middle (2)	Late (3)	Average Stage
Germany	187	0.08**	0.39**	0.74	2.0**
Israel	98	0.93**	0.49**	0.28**	1.4**
Japan	57	0.15**	0.19**	0.65**	2.5**
UK	140	0.48	0.84	0.80	2.1

Panel B: VC Investments by Industry

	Funds	Life Sciences	IT and Software	Elect and Semi-C.	Mfg and Chemicals	Other Industries
Germany	183	0.21**	0.23	0.16	0.23	0.17
Israel	95	0.24**	0.51**	0.16	0.08**	0.01**
Japan	56	0.26**	0.49**	0.05**	0.06**	0.14
UK	140	0.17	0.26	0.15	0.24	0.19

Panel C: Percentage of Funds Investing in Certain Number of Industries

	1	2	3	4 or more
Germany	9%	16%	15%	60%
Israel	39%	23%	17%	21%
Japan	3%	12%	42%	42%
UK	11%	7%	7%	75%

(a)

2 Susan Bull

17 students taking an MSc in Human Centred Systems took part. 8 had taken an MSc module in User Modelling. All had Pocket PCs. 10 undergraduate students taking a degree in Computer Interactive Systems, who had completed undergraduate modules on Personalisation and Adaptive Systems and Interactive Learning Environments, voluntarily took part. Data was obtained by anonymous questionnaire from all subjects, and anonymous logbooks on Pocket PC use over 6 weeks from MSc students. Due to the low numbers it is inappropriate to perform a statistical analysis of the results: the aim is to discover if initial data indicates further work to be valuable.

2.1 Results

Location-Aware User Modelling System. Logbook data shows the most common location of Pocket PC use to be at home, followed by various rooms in EEC/E. Some students also used their Pocket PC in other parts of the campus and elsewhere. Results of 3 typical users are presented in Table 1, as an example of similarities and differences between Pocket PC use. 10 of the generally common activities are listed: reading, email, web browsing, notes, calculator, computer assisted learning, word processing, calculator, music, games. Each user also performed a few additional tasks in other categories, not shown (e.g. MSN Messenger, Excel, viewing lecture slides).

Table 1: Activities and location of use of Pocket PC by 3 students

Location	read	mail	web	notes	calc	CLAL	WP	calc	mus	game
S1 home	1	2	3	4	2	2	1	7	1	
EECE-G16	1	2	1	4	1			1		
EECE-337	1	1	1					1	2	
EECE-421	1	1							1	
EECE-455			2					2		
EECE-CR	1	3	3							
EECE-IB	3	1	1	1					1	
main:lib		3	1	1	1					
shop				4				1		
S2 home	1	4	3	1	4	2	2	7	3	
other:home	1	1	1	1	1	1	1	1		
EECE-123	1	1	1							
EECE-337	5								1	
EECE-522			1	1						
EECE-CR	1									
EECE-IB								1		
EECE-rec	1	2								
EECE-nc	1			1						
campus										
restaurant	1			1				1		
train	5							1	1	
S3 home	1	1	20	4	2			4	8	
EECE-225	1	2								
EECE-337	1	2								
EECE-421	1	1	9					1	1	
laptop:centre			1	1						

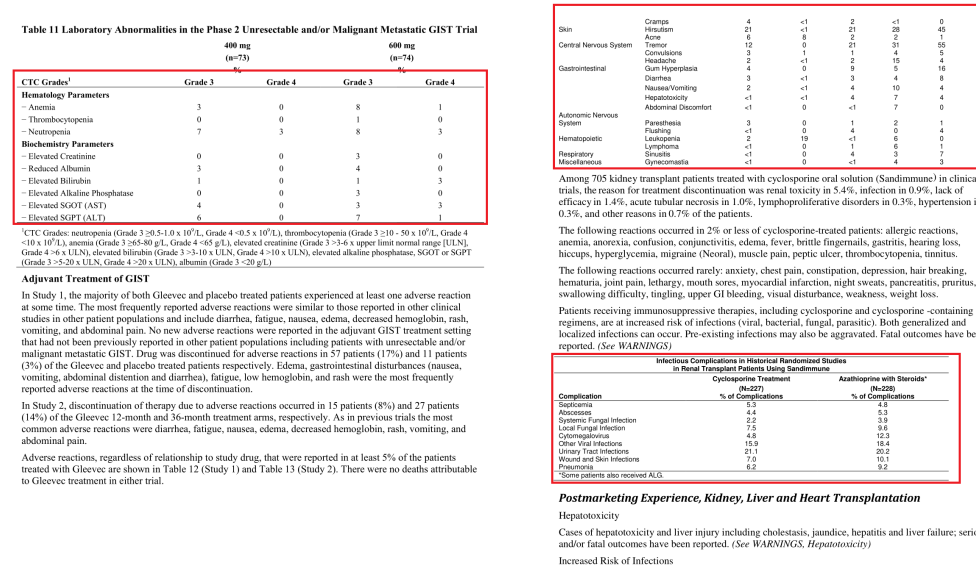
(b)

Figure 13: Examples of images in Marmot

4.1.12. TableBank

The TableBank [61] proposed a novel weak supervision approach for automatically creating the dataset, which is orders of magnitude larger than existing human-labeled datasets for table analysis. Unlike the traditional weakly supervised training set, this approach can generate not only large amounts of but also high-quality training data. There are many electronic documents available on the internet nowadays, such as Microsoft Word (.docx) and LaTeX (.tex) files. By definition, these online documents contain mark-up tags for tables in their source code. Intuitively, these source codes manipulate by adding bounding boxes within each document using the mark-up language. The Office XML code for Word documents can be modified to identify the borderline of each table. The code for Latex documents can also be modified to recognize table bounding boxes. This method generates high-quality labeled data for a wide range of domains, including business documents, official

filings, research papers, and so on, which is extremely useful for large-scale table analysis tasks. The TableBank dataset is made up of 417,234 high-quality labeled tables and their original documents from a variety of domains. A few samples from this dataset are shown in Figure 14.



Reference ID: 3511243

Reference ID: 3722656

(a)

(b)

Figure 14: Examples of images in TableBank

4.1.13. DeepFigures

DeepFigures [62] uses no human assistance to generate high-quality training labels for the task of figure extraction in a huge number of scientific papers. authors do this by locating figures and captions in the rasterized PDF using supplementary data from two big web collections of scientific articles (PubMed and arXiv). authors provide the resulting dataset of approximately 5.5 million tables and figures induced labels to facilitate the development of modern data-driven approaches for this task, which is 4,000 times larger than the previous largest figure extraction dataset and has an average precision of 96.8%. Samples from this dataset are shown in Figure 15.

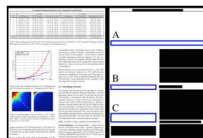


Figure 4. Disambiguating caption to empty space pairing. From the original document (left panel, page from Ouzi and others 2011) text regions and caption regions are detected (shown as filled and empty boxes in the right panel). At this point it is ambiguous what space to assign to the middle caption, labelled as ‘B’, because considered in isolation this caption could plausibly refer to the region above or the region below it. However our algorithm detects that the lower caption, caption C, only has one large, empty region of space nearby that it could refer to. Once it is known that that space has to be assigned to caption C, it becomes clear caption B must be referring to the region above it.

based on how likely it is to contain a figure. Our scoring function rejects regions that contain only empty pixels, or if they are too small. Otherwise regions are scored based on their size, plus a bonus if they contain a large graphical region and a smaller bonus if they contain a smaller graphical region or many different graphical regions. This heuristic helps us to be robust to errors in the previous steps. For example, if a caption has a line plot above it and a bulleted list below it (that was classified as image text), our scoring function will find it preferable to select the line plot’s region over the bulleted list’s region as that caption’s figure region. However if no image regions are found, for example, if the caption really is about a bulleted list, the scoring function will then allow captions to be assigned to regions that contain nothing but text.

Region selection determines which of the proposed regions to select for each caption. A naive approach would be to iterate through each caption and select its highest scoring region, however this can lead to errors in the face of ambiguities. Consider Figure 4, where captions are adjacent to multiple figures making it impossible to judge which region to assign to each caption when considered in isolation. To deal with such ambiguity we iterate over all possible matchings of accepted figure regions to captions and select the highest scoring configuration. In practice the number of possible configurations is almost always very small. Even then 5) since most pages have only a few figures on them, and each figure typically only has a few proposed figure regions that do not get rejected by the scoring function. Use of this strategy for figure-caption assignment rather than iteratively assigning the highest scoring proposal to its corresponding caption increases our precision by about 2.5% and recall by about

	Precision	Recall	F1
Ours	0.957	0.915	0.936
Pnarczyk and Nogueira-bo	0.624	0.500	0.555
Collinsage	0.198	0.116	0.146

Table 1: Precision and recall on figure extraction.

	Precision	Recall	F1
Ours	0.952	0.927	0.939
Pnarczyk and Nogueira-bo	0.429	0.363	0.391

Table 2: Precision and recall on table extraction.

1.5% in our analysis.

A troublesome case for our region proposal method is when figures are directly adjacent to each other, in which case it is difficult to tell where one figure ends and where the other one begins. This is shown in Figure 3. In these cases proposed regions might get expanded too much and include multiple figures. To handle this problem, during the region selection stage, if we detect proposed regions would overlap, an attempt is made to split the conflicting region based on areas of whitespace inside the overlap. We found this increases our recall by about 2%.

4 Dataset

We have assembled a new dataset of 150 documents from three popular computer science conferences. We gathered 50 papers from NIPS 2008-2013, 50 from ICMJ, 2009-2014, and 50 from AAAI 2009-2014 by selecting 10 published papers at random from each conference and year. Annotations were asked to mark bounding regions for each figure and caption using LabelMe². For each region marked by annotations we found the bounding box that contained all foreground pixels within that region. These bounding boxes were then used as ground truth labels. In total we acquired bounding boxes for 458 figures and 194 tables. Our dataset along with the annotations can be downloaded at piffing.usc.edu/figs. We hope our new dataset and ground truth annotations will provide an avenue for researchers to develop their algorithms and make comparisons.

5 Results

We assess our proposed algorithm on our dataset and compare its performance to previous methods. We expect the system being evaluated to return, for each figure extracted, a bounding box for both the figure and its caption as well as the identifier of that figure (e.g., ‘Figure 1’ or ‘Table 7’) and the page number that the figure resides on. Figures with identifiers that did not exist in the hand built labels, or with incorrect page numbers, are considered incorrect. Otherwise a figure is judged by comparing the bounding boxes returned against the ground truth using the overlap score criterion from Everingham and others 2010). Boxes are scored based on the area intersection of the ground truth bounding box and the output bounding box divided by the area of the union between them. If the overlap score exceeds 0.90, we consider the output box to be correct, otherwise it is marked as incorrect. Caption box regions are scored using the same

²<http://labelme2.csail.mit.edu/labelme3/0/index.php>

Figure 15: Examples of images in DeepFigures

4.1.14. PubTables-1M

PubTables-1M [63] contains nearly one million tables from scientific articles, supports multiple input modalities and contains detailed header and location information for table structures, making it useful for a wide variety of modeling approaches. It also addresses a significant source of ground truth inconsistency observed in prior datasets called over-segmentation, using a novel canonicalization procedure. We demonstrate that these improvements lead to a significant increase in training performance and a more reliable estimate of model performance at evaluation for table structure recognition. Further, authors show that transformer-based object detection models trained on PubTables-1M produce excellent results for all three tasks of detection, structure recognition, and functional analysis without the need for any special customization for these tasks. Figure 16 illustrates two examples of this dataset.

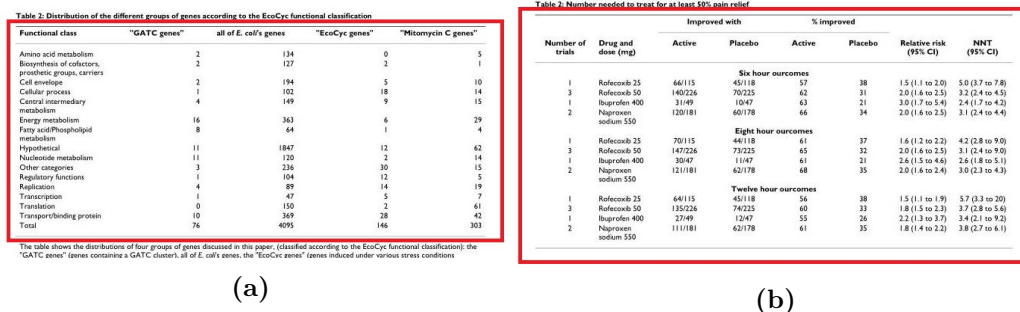


Figure 16: Examples of images in PubTables-1M

4.1.15. SciTSR

SciTSR [64] presents a large-scale table structure recognition dataset derived from scientific articles that comprise 15,000 tables from PDF files and their related structural labels. Figure 17 illustrates two examples of this dataset.

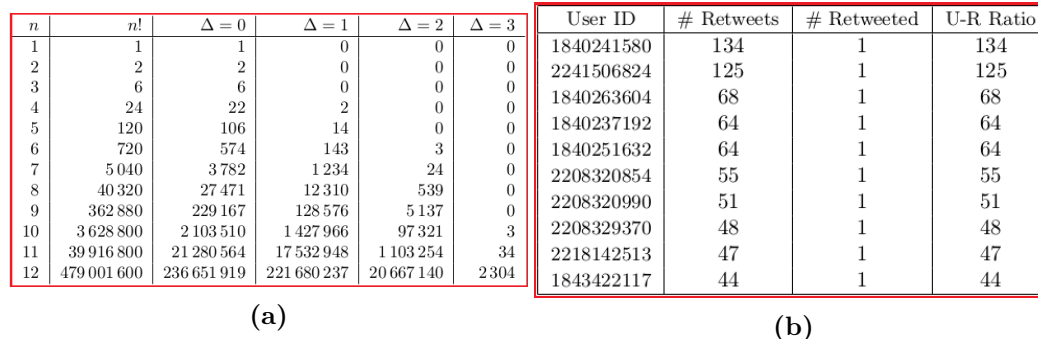


Figure 17: Examples of images in SciTSR

4.1.16. FinTabNet

FinTabNet [65] introduces GTE, a vision-guided systematic framework for combined table detection and cell structured identification that can be constructed on top of any object detection model. Create a new penalty based on the natural cell containment constraint of tables with GTE-Table to train their table network with the help of cell location predictions. GTE-Cell is a novel hierarchical cell detection network that uses table layouts to detect cells. Build a technique for automatically labeling table and cell

structures in existing texts to create a huge corpus of training and test data for a low cost. FinTabNet is a collection of real-world and complicated scientific and financial datasets with thorough table structure annotations to aid in structure identification training and testing. Figure 18 illustrates two examples of this dataset.

NOTES TO CONSOLIDATED FINANCIAL STATEMENTS

NOTE 7: LEASES

We utilize certain aircraft, land, facilities, retail locations and equipment under capital and operating leases that expire at various dates through 2028. We leased 9% of our total aircraft fleet under operating leases as of May 31, 2017 and 10% as of May 31, 2016. A portion of our supplemental aircraft are leased by us under agreements that provide for cancellation upon 30 days' notice. Our leased facilities include national, regional and metropolitan sorting facilities, retail facilities and administrative buildings. Rent expense under operating leases for the years ended May 31, 2017 is as follows (in millions):

	2017	2016	2015
Minimum rentals	\$2,214	\$2,294	\$2,249
Contingent rentals ⁽¹⁾	178	214	184
	\$2,392	\$2,508	\$2,433

⁽¹⁾ Contingent rentals are based on equipment usage.

A summary of future minimum lease payments under noncancelable operating leases with an initial or remaining term in excess of one year at May 31, 2017 is as follows (in millions):

	Aircraft and Related Equipment	Facilities and Other	Total Operating Leases
2018	\$ 398	\$ 2,047	\$ 2,445
2019	343	1,887	2,230
2020	261	1,679	1,940
2021	203	1,506	1,709
2022	185	1,255	1,540
Thereafter	175	2,844	4,019
Total	\$ 1,565	\$ 13,209	\$ 14,774

Property and equipment recorded under capital leases and future minimum lease payments under capital leases are immaterial. The weighted-average remaining lease term of all operating leases outstanding at May 31, 2017 was approximately six years. While certain of our lease agreements contain covenants governing the use of the leased assets or require us to maintain certain levels of insurance, none of our lease agreements include material financial covenants or limitations. FedEx Express makes payments under certain leveraged operating leases that are sufficient to pay principal and interest on certain pass-through certificates. The pass-through certificates are not direct obligations of, or guaranteed by, FedEx Express. We are the lessee under certain operating leases covering a portion of our leased aircraft in which the lessors are trusts established specifically to purchase, finance and lease these aircraft to us. These leasing entities are variable interest entities. We are not the primary beneficiary of the leasing entities, as the lease terms are at market at the inception of the lease and do not include a residual value guarantee, fixed price purchase option or similar feature that obligates us to absorb decreases in value or entitles us to participate in increases in the value of the aircraft. As such, we are not required to consolidate the entity as the primary beneficiary. Our maximum exposure under these leases is included in the summary of future minimum lease payments.

NOTE 8: PREFERRED STOCK

Our Certificate of Incorporation authorizes the Board of Directors, at its discretion, to issue up to 4,000,000 shares of preferred stock. The stock is issuable in series, which may vary as to certain rights and preferences, and has no par value. As of May 31, 2017, none of these shares had been issued.

Table Number	Description	Document Type	Date
3.01	Third Amended and Restated Certificate of Incorporation of Registrant as filed August 24, 2004	Registration Statement on Form S-1, as amended (File No. 333-114984)	August 9, 2004
3.02	Amended and Restated Bylaws of Registrant, effective as of August 24, 2004	Registration Statement on Form S-1, as amended (File No. 333-114984)	August 9, 2004
4.01	Investor Rights Agreement dated May 31, 2002	Registration Statement on Form S-1, as amended (File No. 333-114984)	April 29, 2004
4.01.1	Amendment to Investor Rights Agreement dated August 17, 2004	Registration Statement on Form S-1, as amended (File No. 333-114984)	August 18, 2004
4.02	Specimen Class A Common Stock certificate	Registration Statement on Form S-1, as amended (File No. 333-114984)	August 18, 2004
4.03	Specimen Class B Common Stock certificate	Registration Statement on Form S-1, as amended (File No. 333-114984)	August 18, 2004
4.04	Registration Rights Agreement dated October 9, 2006 (with stockholders of YouTube, Inc.)	Registration Statement on Form S-3 (File No. 333-140498)	February 7, 2007
10.01	Form of Indemnification Agreement entered into between Registrant, its officers and its directors and officers	Registration Statement on Form S-1, as amended (File No. 333-114984)	July 12, 2004
10.02	1998 Stock Plan, as amended	Quarterly Report on Form 10-Q	August 9, 2006
10.03	Applied Semantics, Inc. 1999 Stock Option/Stock Issuance Plan, as amended	Quarterly Report on Form 10-Q	August 9, 2006
10.04	2000 Stock Plan, as amended	Quarterly Report on Form 10-Q	August 9, 2006
10.05	2003 Stock Plan, as amended	Quarterly Report on Form 10-Q	August 9, 2006
10.06	2003 Stock Plan (No. 2), as amended	Quarterly Report on Form 10-Q	August 9, 2006
10.07	2003 Stock Plan (No. 3), as amended	Quarterly Report on Form 10-Q	August 9, 2006
10.08	Google Inc. 2004 Stock Plan, as amended	Current Report on Form 8-K	May 16, 2007
10.08.1	2004 Stock Plan - Stock Option Agreement	Annual Report on Form 10-K	March 30, 2007
10.08.2	2004 Stock Plan - Restricted Stock Unit Agreement	Annual Report on Form 10-K	March 30, 2007
10.09	Lighter Logic, Inc. 2003 Equity Incentive Plan, as amended	Quarterly Report on Form 10-Q	August 9, 2006
10.10	Lifescope Solutions, Inc. 2003 Stock Plan, as amended	Quarterly Report on Form 10-Q	August 9, 2006
10.11	Keyhole, Inc. 2000 Equity Incentive Plan, as amended	Quarterly Report on Form 10-Q	August 9, 2006
10.12	Picasa, Inc. Employee Bonus Plan	Registration Statement on Form S-8 (File No. 333-119758)	September 29, 2004
10.13	YouTube, Inc. 2005 Stock Plan	Registration Statement on Form S-8 (File No. 333-138848)	November 20, 2006
10.14	ProShare Share Agreement dated June 9, 2006 by and among WXIII(Amphibious Realty, L.L.C., WXIII/Citiredux Realty A/R, L.L.C., WXIII/Citiredux Realty C, L.L.C., and WXIII/Citiredux Realty D, L.L.C.) and Google Inc.	Quarterly Report on Form 10-Q	August 9, 2006
10.15	Amended and Restated License Agreement dated October 13, 2003 by and between The Board of Trustees of the Leland Stanford Junior University and Registrant	Registration Statement on Form S-1, as amended (File No. 333-114984)	August 16, 2004
10.15.1	License Agreement dated July 2, 2001 by and between The Board of Trustees of the Leland Stanford Junior University and Registrant	Registration Statement on Form S-1, as amended (File No. 333-114984)	August 18, 2004
10.16	2006 Senior Executive Bonus Plan	Current Report on Form 8-K	October 5, 2006
10.17	License agreement between the Company and Shirley Telfman dated August 16, 2005.	Current Report on Form 8-K	October 6, 2005
10.18	Amended and Restated Limited Liability Company Agreement of AOL Holdings LLC dated March 24, 2006	Annual Report on Form 10-K	March 16, 2006

(a) (b)

Figure 18: Examples of images in FinTabNet

4.1.17. PubTabNet

PubTabNet [66] one of the biggest openly accessible table recognition collection, including 568k table pictures and structured HTML representations. PubTabNet is built automatically by comparing the XML and PDF formats of scientific publications in the PubMed Central™ Open Access Subset (PMCOA). authors also suggest an attention-based encoder-decoder (EDD) architecture for converting table graphics to HTML code. A structure decoder is included in the model, which reconstructs the table structure and assists the cell decoder in recognizing cell content. Furthermore, authors also propose a new Tree-Edit-Distance-based Similarity (TEDS) metric for

table recognition that better captures multi-hop cell misalignment and OCR errors than the existing metric. Figure 19 illustrates two examples of this dataset.

Presenting complaints	N (% of total sample n = 259288)	N (% of each presenting complaint)					
		*Pulse	*BP	*T°C	*GCS	*RR	*SpO ₂
Fever	2154 (0.8)	964 (21.6)	965 (22.0)	1238 (28.7)	1170 (27.1)	2097 (48.1)	1288 (61.1)
Injury (non-head/face/neck)	2995 (1.1)	2767 (9.3)	3300 (10.8)	2583 (8.7)	441 (1.5)	2267 (7.6)	1437 (4.8)
Abdominal pain	23170 (8.9)	5886 (25.4)	5986 (25.8)	4516 (19.5)	311 (1.3)	1520 (6.6)	732 (3.2)
Chest pain	20130 (7.8)	8630 (42.9)	9076 (45.1)	7008 (34.8)	1371 (6.8)	5157 (25.6)	1489 (7.0)
Injury (head/face/neck)	13009 (5.0)	1769 (13.6)	2064 (15.5)	3609 (27.5)	394 (3.0)	1418 (10.7)	852 (6.4)
Nausea	10209 (3.9)	3135 (29.5)	3372 (31.7)	2508 (24.6)	211 (2.0)	3098 (30.0)	400 (3.7)
Headache	9516 (3.7)	3267 (34.3)	3706 (38.9)	2779 (29.2)	286 (3.0)	887 (9.3)	271 (2.8)
Shortness of breath	8548 (3.3)	2711 (31.7)	3087 (36.1)	1936 (22.6)	219 (2.6)	1436 (16.8)	611 (7.2)
Back pain	8239 (3.2)	1557 (18.9)	1597 (19.4)	1392 (16.9)	39 (0.5)	368 (4.5)	169 (2.1)
Diarrhea	1954 (0.8)	1835 (93.8)	1910 (97.2)	1588 (80.7)	108 (5.5)	608 (30.2)	244 (12.3)
Total	160144	41521 (25.8)	43649 (27.0)	38507 (24.0)	4350 (2.8)	18356 (11.5)	7819 (4.7)

Variable	Male		Female	
	%	95% CI	%	95% CI
Sensitivity	39.13	31.55 to 47.12	37.50	30.49 to 44.92
Specificity	93.92	92.68 to 95.00	92.42	91.18 to 93.54
Positive Likelihood Ratio	6.45	4.92 to 8.41	4.95	3.89 to 6.29
Negative Likelihood Ratio	0.65	0.57 to 0.73	0.68	0.60 to 0.76
Disease prevalence	8.61	7.37 to 9.97	8.36	7.23 to 9.59
Positive Predictive Value	37.72	30.35 to 45.54	31.08	25.04 to 37.63
Negative Predictive Value	94.25	93.04 to 95.31	94.19	93.07 to 95.18

(a)

(b)

Figure 19: Examples of images in PubTabNet

4.1.18. TNCR

TNCR [67] a new table collection containing images of varied quality gathered from free access websites The TNCR dataset may be used to recognize tables in scanned document pictures and classify them into five categories. TNCR has roughly 6621 photos and 9428 captioned tables. To build numerous robust baselines, this work used state-of-the-art deep learning-based approaches for table detection. On the TNCR dataset, Deformable DERT with Resnet-50 Backbone Network delivers the best results compared to other methods, with an accuracy of 86.7%, recall of 89.6%, and f1 score of 88.1%. A few samples from this dataset are shown in Figure 20.

4.1.19. SynthTabNet

To correct an imbalance in the earlier datasets, A Nassar [68] proposes SynthTabNet, a synthetically created dataset with a variety of appearance styles and complexity. The authors have created four synthetic datasets, each with 150k samples. The most common words from PubTabNet and FinTabNet as well as randomly produced text make up the corpora used to create the table content. The first two synthetic datasets have been adjusted to closely resemble the look of the real datasets while incorporating more intricate table structures. The third one adopts a colorful style with strong contrast, while the final one has tables with little content. Last but not least, The authors have integrated all synthetic datasets into a single, 600k-example synthetic dataset. A few samples from this dataset are shown in Figure 21.

Table 11 Laboratory Abnormalities in the Phase 2 Unresectable and/or Malignant Metastatic GIST Trial

CTC Grades ¹	400 mg (n=73)		600 mg (n=74)	
	Grade 3	Grade 4	Grade 3	Grade 4
Hematology Parameters				
- Anemia	3	0	8	1
- Thrombocytopenia	0	0	1	0
- Neutropenia	7	3	8	3
Biochemistry Parameters				
- Elevated Creatinine	0	0	3	0
- Reduced Albumin	3	0	4	0
- Elevated Bilirubin	1	0	1	3
- Elevated Alkaline Phosphatase	0	0	3	0
- Elevated SGOT (AST)	4	0	3	0
- Elevated SGPT (ALT)	4	0	7	1

¹CTC Grades: neutropenia (Grade 3 $\geq 5.1 \times 10^9/L$, Grade 4 $< 0.5 \times 10^9/L$), thrombocytopenia (Grade 3 $20 - 50 \times 10^9/L$, Grade 4 $< 10 \times 10^9/L$), anemia (Grade 3 $65-80 g/L$, Grade 4 $< 65 g/L$), elevated creatinine (Grade 3 $> 3-6 \times$ upper limit normal range [ULN], Grade 4 $> 6 \times$ ULN), elevated bilirubin (Grade 3 $> 3-10 \times$ ULN, Grade 4 $> 10 \times$ ULN), elevated alkaline phosphatase, SGOT or SGPT (Grade 3 $> 5 \times 20 \times$ ULN, Grade 4 $> 20 \times$ ULN), albumin (Grade 3 $> 20 g/L$)

Adjuvant Treatment of GIST

In Study 1, the majority of both Gleevec and placebo treated patients experienced at least one adverse reaction at some time. The most frequently reported adverse reactions were similar to those reported in other clinical studies in other patient populations and include diarrhea, fatigue, nausea, edema, decreased hemoglobin, rash, vomiting, and abdominal pain. No new adverse reactions were reported in the adjuvant GIST treatment setting that had not been previously reported in other patient populations including patients with unresectable and/or malignant metastatic GIST. Drug was discontinued for adverse reactions in 57 patients (17%) and 11 patients (3%) of the Gleevec and placebo treated patients respectively. Edema, gastrointestinal disturbances (nausea, vomiting, abdominal distention and diarrhea), fatigue, low hemoglobin, and rash were the most frequently reported adverse reactions at the time of discontinuation.

In Study 2, discontinuation of therapy due to adverse reactions occurred in 15 patients (8%) and 27 patients (14%) of the Gleevec 12-month and 36-month treatment arms, respectively. As in previous trials the most common adverse reactions were diarrhea, fatigue, nausea, edema, decreased hemoglobin, rash, vomiting, and abdominal pain.

Adverse reactions, regardless of relationship to study drug, that were reported in at least 5% of the patients treated with Gleevec are shown in Table 12 (Study 1) and Table 13 (Study 2). There were no deaths attributable to Gleevec treatment in either trial.

Reference ID: 3511243

(a)

Cramps	4	<1	2	<1	0
Skin					
Hitching	21	<1	21	28	45
Alope	6	8	2	2	1
Central Nervous System					
Tremor	12	0	21	31	55
Convulsions	3	1	1	4	5
Headache	2	<1	2	15	4
Gastrointestinal					
Gum Hyperplasia	4	0	8	5	16
Diarrhea	3	<1	3	4	8
Nausea/Vomiting	2	<1	4	10	4
Hepatotoxicity	<1	<1	4	7	4
Autonomic Nervous System					
Abdominal Discomfort	<1	0	<1	7	0
Paresthesia	3	0	1	2	1
Flushing	<1	0	4	0	4
Hematopoietic					
Leucopenia	2	19	<1	6	0
Lymphoma	<1	0	1	5	1
Respiratory					
Syncope	<1	0	4	5	7
Musculoskeletal					
Osteonecrosis	<1	0	<1	3	3

Among 705 kidney transplant patients treated with cyclosporine oral solution (Sandimmune[®]) in clinical trials, the reason for treatment discontinuation was renal toxicity in 5.4%, infection in 0.9%, lack of efficacy in 1.4%, acute tubular necrosis in 1.0%, lymphoproliferative disorders in 0.3%, hypertension in 0.3%, and other reasons in 0.7% of the patients.

The following reactions occurred in 2% or less of cyclosporine-treated patients: allergic reactions, anemia, anorexia, confusion, conjunctivitis, edema, fever, brittle fingernails, gastritis, hearing loss, hiccups, hyperglycemia, migraine (Neoral), muscle pain, peptic ulcer, thrombocytopenia, tinnitus.

The following reactions occurred rarely: anxiety, chest pain, constipation, depression, hair breaking, hematuria, joint pain, lethargy, mouth sores, myocardial infarction, night sweats, pancreatitis, pruritus, swallowing difficulty, tingling, upper GI bleeding, visual disturbance, weakness, weight loss.

Patients receiving immunosuppressive therapies, including cyclosporine and cyclosporine-containing regimens, are at increased risk of infections (viral, bacterial, fungal, parasitic). Both generalized and localized infections can occur. Pre-existing infections may also be aggravated. Fatal outcomes have been reported. (See **WARNINGS**).

Complication	Cyclosporine Treatment (N=27)		Azathioprine with Steroids ^a (N=29)	
	% of Complications	% of Complications	% of Complications	% of Complications
Sepsis	5.5	4.5		
Abscesses	4.4	5.3		
Systemic Fungal Infection	2.2	3.9		
Local Fungal Infection	7.5	9.6		
Cytomegalovirus	4.8	12.9		
Other Viral Infections	15.9	18.4		
Urinary Tract Infections	21.1	29.2		
Wound and Skin Infections	7.0	10.1		
Pneumonia	6.2	5.2		

^aSome patients also received ALG.

Postmarketing Experience, Kidney, Liver and Heart Transplantation

Hepatotoxicity

Cases of hepatotoxicity and liver injury including cholestasis, jaundice, hepatitis and liver failure; serious and/or fatal outcomes have been reported. (See **WARNINGS, Hepatotoxicity**)

Increased Risk of Infections

Reference ID: 3722856

(b)

Figure 20: Examples of images in TNCR

XBRL Taxonomy Extension Schema Document	P-2	Balance, beginning of period	Treasury Stock	Cost of revenue	Balance at December 31, 2015
Pinnacle West APS	Total loans and leases	Years ended December 31,			
Entergy Mississippi	Balance at end of period	Repurchase of common stock	Selling, general and administrative expenses	Income tax expense	New York
†	452264	41216	174676	9986	579181
Other, net	143261	476128	499421	785493	919778
Years Ended December 31,	308084	359700	722933	797841	
High	644715	152726	919140	193062	631013
Level 3	471056	860113	989378		
Total long-term debt	516184	596264	739835	882032	770620
Accumulated benefit obligation	778529	779405		330204	190206
Fiscal Year	288049	160223		981515	623850

(a)

N	No.	Mean SD	N	Type
Sample	6.71%	77.35%	62.77%	0.60%
Characteristic	8.5%	47.27%	59.49%	97.29%
References				
Cases	66.89%	70.26%	1.77%	68.38%
		44.64%	57.81%	47.24%
N	38.4%	92.19%	71.28%	31.51%
Factor	95.45%	26.42%	66.94%	14.62%
df	14.8%	34.61%		7.32%
Median	85.41%	64.48%	18.51%	24.75%
No.	35.63%	52.37%	75.63%	20.10%
Number	94.87%	69.32%	29.92%	0.23%
Mean	37.21%	24.33%	45.89%	

(b)

Figure 21: Examples of images in SynthTabNet

Table 1 presents a comparison between some of the popular datasets of table detection and structure recognition.

Table 1: The table illustrates a quantitative comparison between some famous datasets in table detection.

Dataset	Total pages	Total Tables	Table detection	Table Structure	Classification	Scanned
ICDAR2013	462	150	✓	✓	✗	✓
ICDAR2017-POD	2,417	-	✓	✗	✗	✓
TabStructDB	2.4k	-	✗	✓	✗	✓
TABLE2LATEX-450K	-	450,000	✗	✓	✗	✓
RVL-CDIP (SUBSET)	518	-	✓	✗	✗	✓
IIT-AR-13K	13K	-	✓	✗	✗	✓
CamCap	85	-	✓	✓	✗	✗
UNLV	2889	-	✓	✓	✗	✓
UW-3 dataset	1600	-	✓	✓	✗	✓
Marmot	2000	-	✓	✗	✗	✓
TableBank	-	417,234	✓	✗	✗	✓
ICDAR2019	-	2000	✓	✓	✗	✓
DeepFigures	-	5.5 million	✓	✗	✗	✓
PubTables-1M	460,589	1 million	✓	✓	✗	✓
SciTSR	-	15,000	✗	✓	✗	✗
FinTabNet	89,646	112,887	✓	✓	✗	✗
PubTabNet	-	568k	✗	✓	✗	✓
TNCR	6621	9428	✓	✗	✓	✓
SynthTabNet	600k	-	✓	✓	✓	✓

4.2. Metrics

Table detectors use multiple criteria to measure the performance of the detectors viz., frames per second (FPS), precision, and recall. However, mean Average Precision (mAP) is the most common evaluation metric. Precision is derived from Intersection over Union (IoU), which is the ratio of the area of overlap and the area of union between the ground truth and the predicted bounding box. A threshold is set to determine if the detection is correct. If the IoU is more than the threshold, it is classified as True Positive while an IoU below it is classified as False Positive. If the model fails to detect an object present in the ground truth, it is termed a False Negative. Precision measures the percentage of correct predictions while recall measures the correct predictions with respect to the ground truth.

$$\begin{aligned}
 \text{Average Precision (AP)} &= \frac{\text{True Positive (TP)}}{(\text{True Positive (TP)} + \text{False Positive (FP)})} \quad (4) \\
 &= \frac{\textit{TruePositive}}{\textit{AllObservations}}
 \end{aligned}$$

$$\begin{aligned} \text{Average Recall (AR)} &= \frac{\text{True Positive (TP)}}{(\text{True Positive (TP)} + \text{False Negative (FN)})} \\ &= \frac{\textit{TruePositive}}{\textit{AllGroundTruth}} \end{aligned} \quad (5)$$

$$\text{F1-score} = \frac{2 * (\text{AP} * \text{AR})}{(\text{AP} + \text{AR})} \quad (6)$$

Based on the above equation, average precision is computed separately for each class. To compare performance between the detectors, the mean of average precision of all classes, called mean average precision (mAP) is used, which acts as a single metric for final evaluation.

IOU is a metric that finds the difference between ground truth annotations and predicted bounding boxes. This metric is used in most state of art object detection algorithms. In object detection, the model predicts multiple bounding boxes for each object and based on the confidence scores of each bounding box it removes unnecessary boxes based on their threshold value. We need to declare the threshold value based on our requirements.

$$\text{IOU} = \frac{\text{Area of union}}{\text{area of intersection}} \quad (7)$$

5. Table detection and structure recognition Models

Table detection has been studied for an extended period of time. Researchers used different methods that can be categorized as follows:

1. heuristic-based methods
2. machine learning-based methods
3. deep learning-based methods

Primarily heuristic-based methods were mainly used in the 1990s, 2000s, and early 2010. They employed different visual cues like lines, keywords, space features, etc. to detect tables.

P. Pyreddy et al. [69] proposed an approach of detecting tables using character alignment, holes, and gaps. Wang et al. [70]. used a statistical approach to detect table lines depending on the distance between consecutive words. Grouped horizontal consecutive words together with vertical adjacent lines were employed to propose table entity candidates. Jahan et al. [71]

presented a method that uses local thresholds for word spacing and line height for detecting table regions.

Itonori [72] proposed a rule-based approach that led to the text-block arrangement and ruled line position to localize the table in the documents. Chandran and Kasturi [73] developed another table detection approach based on vertical and horizontal lines. Wonkyo Seo et al. [56] used junctions (intersection of the horizontal and vertical line) detection with further processing.

Hassan et al. [74] locate and segment tables by analyzing spatial features of text blocks. Ruffolo et al. [75] introduced PDF-TREX, a heuristic bottom-up approach for table recognition in single-column PDF documents. It uses the spatial features of page elements to align and group them into paragraphs and tables. Nurminen [76] proposed a set of heuristics to locate subsequent text boxes with common alignments and assign them the probability of being a table.

Fang et al. [77] used the table header as a starting point to detect the table region and decompose its elements. Harit et al. [78] proposed a technique for table detection based on the identification of unique table start and trailer patterns. Tupaj et al. [79] proposed an OCR based table detection technique. The system searches for sequences of table-like lines based on the keywords

The above methods work relatively well on documents with uniform layouts. However, heuristic rules need to be tweaked to a wider variety of tables and are not really suited for generic solutions. Therefore, machine learning approaches started to be employed to solve the table detection problem.

Machine learning-based methods were common around the 2000s and the 2010s.

Kieninger et al. [80] applied an unsupervised learning approach by clustering word segments. Cesarini et al. [81] used a modified XY tree supervised learning approach. Fan et al. [82] uses both supervised and unsupervised approaches to table detection in PDF documents. Wang and Hu [83] applied Decision tree and SVM classifiers to layout, content type and word group features. T. Kasar et al. [84] used the junction detection and then passed the information to the SVM classifier. Silva et al. [85] applied joint probability distribution over sequential observations of visual page elements (Hidden Markov Models) to merge potential table lines into tables. Klampfl et al. [86] compare two unsupervised table recognition methods from digital scientific articles. Docstrum algorithm [87] applies KNN to aggregate structures into lines and then uses perpendicular distance and angle between lines to combine them into text blocks. It must be noted that this algorithm was

devised in 1993, earlier than other methods mentioned in this section.

F Shafait [88] proposes a useful method for table recognition that performs well on documents with a range of layouts, including business reports, news stories, and magazine pages. The Tesseract OCR engine offers an open-source implementation of the algorithm.

As neural networks gained interest, researchers started to apply them to document layout analysis tasks. Initially, they were used at simpler tasks like table detection. Later on, as more complex architectures were developed, more work was put into table columns and overall structure recognition.

Hao et al. [24] employed CNN to detect whether a certain region proposal is a table or not. Azka Gilani et al. [22] proposed a Faster R-CNN-based model to make up for the limitations of Hao et al. [24] and other prior methodologies.

Sebastian Schreiber et al. [20] were the first to perform table detection and structure recognition using Faster RCNN. He et al. [89], used FCN for semantic page segmentation. S. Arif et al. [90] attempted to improve the accuracy of Faster R-CNN by using semantic color-coding of text. Reza et al. [91] used a combination of GAN-based architecture for table detection. Agarwal et al. [92] used a multistage extension of Mask R-CNN with a dual backbone for detecting tables.

Recently transformer-based models were applied to document layout analysis, Smock, Brandon et al. [63] applied Carion et al.[93] DETection TRansformer framework, a transformer encoder-decoder architecture, to their table dataset for both table detection and structure recognition tasks. Xu et al. [94] proposed a self-supervised pre-trained Document Image Transformer model using large-scale unlabeled text images for document analysis, including table detection

5.1. Table detection Models

In this section, we examine the deep learning methods used for document image table detection. We have divided the methods into several deep learning ideas for the benefit of our readers' convenience. Table 2 lists all the object identification-based table detection strategies. It also discusses various deep learning-based methods that have been used in these methods.

A Gilani [22] has shown how to recognize tables using deep learning. Document pictures are pre-processed initially in the suggested technique. These photos are then sent into a Region Proposal Network for table detection, which is followed by a fully connected neural network. The suggested

approach works with great precision on a variety of document pictures, including documents, research papers, and periodicals, with various layouts.

D Prasad [95] presents an automatic table detection approach for interpreting tabular data in document pictures, which primarily entails addressing two issues: table detection and table structure recognition. Using a single Convolution Neural Network (CNN) model, provide an enhanced deep learning-based end-to-end solution for handling both table detection and structure recognition challenges. CascadeTabNet is a Cascade mask Region-based CNN High-Resolution Network (Cascade mask R-CNN HRNet)-based model that simultaneously identifies table areas and recognizes structural body cells from those tables.

SS Paliwal [96] presents TableNet which is a new end-to-end deep learning model for both table detection and structure recognition. To divide the table and column areas, the model uses the dependency between the twin objectives of table detection and table structure recognition. Then, from the discovered tabular sub-regions, semantic rule-based row extraction is performed.

Y Huang [97] describes a table detecting algorithm based on the YOLO principle. The authors offer various adaptive improvements to YOLOv3, including an anchor optimization technique and two post-processing methods, to account for the significant differences between document objects and real objects. also employ k-means clustering for anchor optimization to create anchors that are more suited for tables than natural objects, making it easier for our model to find the exact placements of tables. The additional whitespaces and noisy page objects are deleted from the projected results during the post-processing procedure.

L Hao [24] offers a new method for detecting tables in PDF documents that are based on convolutional neural networks, one of the most widely used deep learning models. The suggested method begins by selecting some table-like areas using some vague constraints, then building and refining convolutional networks to identify whether the selected areas are tables or not. Furthermore, the convolutional networks immediately extract and use the visual aspects of table sections, while the non-visual information contained in original PDF documents is also taken into account to aid in better detection outcomes.

SA Siddiqui [98] provide a novel strategy for detecting tables in documents. The approach given here takes advantage of data's potential to recognize tables with any arrangement. however, the given method works directly

on photos, making it universally applicable to any format. The proposed method uses a unique mix of deformable CNN and speedier R-CNN/FPN. Because tables might be present at variable sizes and transformations, traditional CNN has a fixed receptive field, which makes table recognition difficult (orientation). Deformable convolution bases its receptive field on the input, allowing it to shape it to match the input. The network can accommodate tables of any layout because of this customization of the receptive field.

N Sun [99] presents a corner-finding approach for faster R-CNN-based table detection. The Faster R-CNN network is first used to achieve coarse table identification and corner location. then, coordinate matching is used to group those corners that belong to the same table. Untrustworthy edges are filtered at the same time. Finally, the matching corner group fine-tunes and adjusts the table borders. At the pixel level, the suggested technique enhances table boundary finding precision.

I Kavasidis[100] propose a method for detecting tables and charts using a combination of deep CNNs, graphical models, and saliency ideas. M Holeček [101] presented the concept of table understanding utilizing graph convolutions in structured documents like bills, extending the applicability of graph neural networks. A PDF document is used in the planned research as well. The job of line item table detection and information extraction are combined in this study to tackle the problem of table detection. Any word may be quickly identified as a line item or not using the line item technique. Following word classification, the tabular region may be easily identified since, in contrast to other text sections on bills, table lines are able to distinguish themselves rather effectively.

Á Casado-García [102] Uses object detection techniques, The authors have shown that fine-tuning from a closer domain improves the performance of table detection after conducting a thorough examination. The authors have utilized Mask R-CNN, YOLO, SSD, and Retina Net in conjunction with object detection algorithms. Two basic datasets are chosen to be used in this investigation, TableBank and PascalVOC.

X Zheng [103] provides Global Table Extractor (GTE), a method for jointly detecting tables and recognizing cell structures that can be implemented on top of any object detection model. To train their table network with the help of cell placement predictions, the authors develop GTE-Table, which introduces a new penalty based on the inherent cell confinement limitation of tables. A novel hierarchical cell identification network called GTE-Cell makes use of table styles. Additionally, in order to quickly and inexpensively

build a sizable corpus of training and test data, authors develop a method to automatically classify table and cell structures in preexisting texts.

Y Li [104] provides a new network to produce the layout elements for table text and to enhance the performance of less ruled table identification. The Generative Adversarial Networks(GAN) and this feature generator model are comparable. The authors mandate that the feature generator model extract comparable features for both heavily governed and loosely ruled tables.

DD Nguyen [105] introduces TableSegNet, a fully convolutional network with a compact design that concurrently separates and detects tables. TableSegNet uses a shallower path to discover table locations in high resolution and a deeper path to detect table areas in low resolution, splitting the found regions into separate tables. TableSegNet employs convolution blocks with broad kernel sizes throughout the feature extraction process and an additional table-border class in the main output to increase the detection and separation capabilities.

D Zhang [106] suggests a YOLO-table-based table detection methodology. To enhance the network's capacity to learn the spatial arrangement aspects of tables, the authors incorporate involution into the network's core, and the authors create a simple Feature Pyramid Network to increase model efficacy. This research also suggests a table-based enhancement technique.

5.2. Table Structure Recognition Models

In order to recognize table structures in document images, deep learning approaches are reviewed in this part. We divided the methods into discrete deep-learning principles for the benefit of our readers. Table 3,4 lists all methods for recognizing table structures based on object detection, as well as their benefits and drawbacks. It also discusses various deep learning-based methods that have been used in these methods.

A Zucker [107] presents CluSTi, a Clustering approach for recognizing the Structure of Tables in invoice scanned images, as an effective way. CluSTi makes three contributions. To begin, it uses a clustering approach to eliminate high noise from the table pictures. Second, it uses state-of-the-art text recognition to extract all text boxes. Finally, CluSTi organizes the text boxes into the correct rows and columns using a horizontal and vertical clustering technique with optimum parameters. Z Zhang [108] present Split, Embed, and Merge (SEM) is a table structure recognizer that is accurate. M Namysl [109] presents a versatile and modular table extraction approach in this research.

Table 2: A comparison of the benefits and drawbacks of several deep learning-based table detection methods

Literature	Method	Benefits	Drawbacks
A Gilani[22]	Faster R-CNN	1) On scanned document pictures, this is the first deep learning-based table detection method. 2) The object detection technique is made easier by converting RGB pixels to distance measures.	There are additional phases in the pre-processing process.
S Schreiber[20]	transfer learning methods + Faster R-CNN	end-to-end strategy for detecting tables and table structures that is straightforward and efficient	When compared to other state-of-the-art techniques, it is less accurate.
SA Siddiqui [98]	Deformable CNN + Faster R-CNN	Deformable convolutional neural networks' dynamic receptive field aids in the reconfiguration of multiple tabular boundaries.	When compared to standard convolutions, deformable convolutions are computationally demanding.
SS Paliwal [96]	Networks with fully convolutions	1) First attempt at combining a single solution to handle both the problem of table detection and structure recognition. 2) A comprehensive method for structure recognition and detection in document pictures.	This approach only functions on column detection when used for table structure extraction.
P Riba [54]	OCR-based Graph NN that makes use of textual characteristics	The suggested technique makes use of more data than only spatial attributes.	1) No comparisons to other state-of-the-art strategies. 2) Additional annotations are needed using this strategy in addition to the tabular data.
N Sun [99]	Faster R-CNN + Locate corners	1) Better outcomes are obtained using a novel technique. 2) Faster R-CNN is used to identify not just tables, but also the corners of tabular borders	1) It is necessary to do postprocessing operations such as corner refining. 2) Because of the additional detections, the computation is more involved.
I Kavasidis [100]	combination of deep CNNs, graphical models, and saliency	1) Dilated convolutions rather than conventional convolutions are used. 2) Using this technique, saliency detection is performed in place of table detection.	To provide equivalent results, many processing stages are necessary.
M Holeček [101]	Graph NN + line item identification Method	This approach yields encouraging outcomes when used to layout-intensive documents like invoices and PDFs.	1) Limited baseline approach without comparisons to other state-of-the-art techniques 2) No publicly accessible table datasets are used for the evaluation of the approach.
Y Huang [97]	YOLO	In comparison, a quicker and more effective strategy	The suggested methodology relies on data-driven post-processing methods.
Y Li [104]	Generative Adversarial Networks(GAN)	For ruling and less ruled tables, the GAN-based strategy drives the network to extract comparable characteristics.	In document images with different tabular layouts, the generator-based model is susceptible.
M Li [61]	Faster R-CNN	This method demonstrates how a basic Faster R-CNN can yield excellent results when used with a huge dataset like TableBank.	Just a simple Faster-RCNN implementation
D Prasad [95]	Cascade mask Region-based CNN High-Resolution Network-based model	The study shows how iterative transfer learning may be used to transform pictures, which can lessen the need on huge datasets.	The same as[22], There are additional phases in the pre-processing process.
Á Casado-García [102]	Like fine-tuning + Mask R-CNN, RetinaNet, SSD and YOLO	Describe the advantages of using object detection networks in conjunction with domain-specific fine-tuning techniques for table detection.	Closed domain fine-tuning is still insufficient to get state-of-the-art solutions.
M Agarwal [92]	multistage extension of Mask R-CNN with a dual backbone	1) A comprehensive object detection-based framework utilizing a composite backbone to deliver state-of-the-art outcomes 2) Extensive tests on benchmark datasets for table detection that are openly accessible.	The technique is computationally expensive since it uses a composite backbone in addition to deformable convolutions.
X Zheng [103]	Global Table Extractor (GTE) which is general method for object detection	1) The problem of table detection is benefited by the extra piece-wise constraint loss introduced. 2) a complete method that is compatible with all object detection frameworks.	Annotations for cellular borders are necessary since the process of table detection depends on cell detection.

E Koci [110] offers a new method for identifying tables in spreadsheets and constructing layout areas after determining the layout role of each cell. Using a graph model, they express the spatial interrelationships between these areas. On this foundation, they present Remove and Conquer (RAC), a table recognition algorithm based on a set of carefully selected criteria.

Using the potential of deformable convolutional networks, SA Siddiqui [51] proposes a unique approach for analyzing tabular patterns in document

pictures. P Riba [54] presents a graph-based technique for recognizing tables in document pictures in this paper. also employ the location, context, and content type instead of the raw content (recognized text), thus it's just a structural perception technique that's not reliant on the language or the quality of the text reading. E Koci [111] use genetic-based techniques for graph partitioning, to recognize the sections of the graph matching to tables in the sheet.

SA Siddiqui [112] described the structure recognition issue as the semantic segmentation issue. To segment the rows and columns, the authors employed fully convolutional networks. The approach of prediction tiling is introduced, which lessens the complexity of table structural identification, assuming consistency in a tabular structure. The author imported pre-trained models from ImageNet and used the structural models of FCN's encoder and decoder. The model creates features of the same size as the original input picture when given an image.

SA Khan [113] presents a robust deep learning-based solution for extracting rows and columns from a recognized table in document pictures in this work. The table pictures are pre-processed before being sent into a bi-directional Recurrent Neural Network using Gated Recurrent Units (GRU) and a fully-connected layer with softmax activation in the suggested solution. SF Rashid [114] provides a new learning-based approach for table content identification in diverse document pictures. SR Qasim [115] presents a graph network-based architecture for table recognition as a superior alternative to typical neural networks. S Raja [116] describes a method for recognizing table structure that combines cell detection and interaction modules to locate the cells and forecast their relationships with other detected cells in terms of row and column. Also, add structural limitations to the loss function for cell identification as extra differential components. The existing issues with end-to-end table identification were examined by Y Deng [52], who also highlighted the need for a larger dataset in this area.

Another study by Y Zou [117] called for the development of an image-based table structure identification technique using fully convolutional networks. the shown work divides a table's rows, columns, and cells. All of the table components' estimated bounds are enhanced using connected component analysis. Based on the placement of the row and column separators, row and column numbers are then allocated for each cell. In addition, special algorithms are used to optimize cellular borders.

To identify rows and columns in tables, KA Hashmi [118] suggested a

guided technique for table structure identification. The localization of rows and columns may be made better, according to this study, by using an anchor optimization approach. The boundaries of rows and columns are detected in their proposed work using Mask R-CNN and optimized anchors.

Another effort to segment tabular structures is the ReS2TIM paper by W Xue [119] which describes the reconstruction of syntactic structures from the table. Regressing the coordinates for each cell is this model’s main objective. A network that can identify the neighbors of each cell in a table is initially built using the new technique. In the study, a distance-based weighting system is given that will assist the network in overcoming the training-related class imbalance problem.

C Tensmeyer [120] has presented SPLERGE (Split and Merge), another method using dilated convolutions. Their strategy entails the use of two distinct deep learning models, the first of which establishes the grid-like layout of the table and the second of which determines if further cell spans over many rows or columns are possible.

A Nassar [68] provide a fresh identification model for table structures. The latter enhances the most recent encoder-dual-decoder from PubTabNet end-to-end deep learning model in two important aspects. First, the authors provide a brand-new table-cell object detection decoder. This allows them to easily access the content of the table cells in programmatic PDFs without having to train any proprietary OCR decoders. The authors claim that this architectural improvement makes table-content extraction more precise and enables them to work with non-English tables. Second, transformer-based decoders take the place of LSTM decoders.

S Raja [121] suggests a novel object-detection-based deep model that is tailored for quick optimization and captures the natural alignments of cells inside tables. Dense table recognition may still be problematic even with precise cell detection because multi-row/column spanning cells make it difficult to capture long-range row/column relationships. Therefore, the authors also seek to enhance structure recognition by determining a unique rectilinear graph-based formulation. The author emphasizes the relevance of empty cells in a table from a semantics standpoint. The authors recommend a modification to a well-liked assessment criterion to take these cells into consideration. To stimulate fresh perspectives on the issue, then provide a moderately large assessment dataset with annotations that are modeled after human cognition.

X Shen [122] suggested two modules, referred to as Rows Aggregated

(RA) and Columns Aggregated (CA). First, to produce a rough forecast for the rows and columns and address the issue of high error tolerance, feature slicing and tiling are applied. Second, the attention maps of the channels are computed to further obtain the row and column information. In order to complete the rows segmentation and columns segmentation, the authors employ RA and CA to construct a semantic segmentation network termed the Rows and Columns Aggregated Network (RCANet).

C Ma[123] present RobusTabNet, a novel method for recognizing the structure of tables and detecting their borders from a variety of document pictures. The authors suggest using CornerNet as a new region proposal network to produce higher quality table proposals for Faster R-CNN, which has greatly increased the localization accuracy of Faster R-CNN for table identification. by utilizing only the minimal ResNet-18 backbone network. Additionally, the authors suggest a brand-new split-and-merge approach for recognizing table structures. In this method, each detected table is divided into a grid of cells using a novel spatial CNN separation line prediction module, and then a Grid CNN cell merging module is used to recover the spanning cells. Their table structure recognizer can accurately identify tables with significant blank areas and geometrically deformed (even curved) tables because the spatial CNN module can efficiently transmit contextual information throughout the whole table picture. B Xiao [124] postulates that a complex table structure may be represented by a graph, where the vertices and edges stand in for individual cells and the connections between them. Then, the authors design a conditional attention network and characterize the table structure identification issue as a cell association classification problem (CATT-Net).

A Jain [125] suggests training a deep network to recognize the spatial relationships between various word pairs included in the table picture in order to decipher the table structure. The authors offer an end-to-end pipeline called TSR-DSAW: TSR through Deep Spatial Association of Words, which generates a digital representation of a table picture in a structured format like HTML. The suggested technique starts by utilizing a text-detection network, such as CRAFT, to identify every word in the input table picture. Next, using dynamic programming, word pairings are created. These word pairings are underlined in each individual image and then given to a DenseNet-121 classifier that has been trained to recognize spatial correlations like same-row, same-column, same-cell, or none. Finally, The authors apply post-processing to the classifier output in order to produce the HTML table structure.

H Li [126] formulate the issue as a cell relation extraction challenge and provide T2, a cutting-edge two-phase method that successfully extracts table structures from digitally preserved texts. T2 offers a broad idea known as a prime connection that accurately represents the direct relationships between cells. To find complicated table structures, it also builds an alignment graph and uses a message-passing network.

6. Methodology

In this section, we will extend the methodology and methods used for the TNCR dataset in our previous work [67]. In the previous work, we described Cascade R-CNN, Cascade Mask R-CNN, Cascade RPN, Hybrid Task Cascade (HTC), YOLO, and Deformable DETR. In this section, we will describe additional four methodologies of using object detection and classification for Faster R-CNN, Mask R-CNN, HRNets, Resnest, and Dynamic R-CNN.

6.1. *Faster R-CNN*

Faster R-CNN [127] contains two modules: The RPN is a fully-convolutional network that generates region proposals, and the Fast-RCNN detector takes the proposal from RPN as input and generates object detection results as seen in Fig. 22. A feature extraction network, which is often a pretrained CNN, is employed in a Faster R-CNN object detection network, similar to what we utilized for its predecessor. Following that, there are two trainable subnetworks. The first is a Region Proposal Network (RPN), which is used to produce object proposals as its name indicates, and the second is used to predict the object’s real class. The RPN that is put after the last convolutional layer is thus the major differentiator for Faster R-CNN. This has been taught to generate region proposals without the use of any external mechanisms such as Selective Search. Then, similar to Fast R-CNN, utilize ROI pooling, an upstream classifier, and a bounding box regressor.

6.2. *Mask R-CNN*

Mask R-CNN [128] uses R-CNN to effectively detect objects in an image while also performing object segmentation tasks for each region of interest. As a result, segmentation runs concurrently with classification and bounding box regression. The high-level architecture of the Mask R-CNN is shown in Fig. 23. Mask RCNN is divided into two phases. First, it generates proposals based on the input image for regions where an object might be

Table 3: A comparison of the benefits and drawbacks of several deep learning-based table Structure recognition methods

Literature	Method	Benefits	Drawbacks
SF Rashid [114]	Uses the geometric position of words + A neural network model (autoMLP)	No reliance on complex layout analysis Mechanism. Can be used on the diverse set of documents with different layouts	limitation is in marking columns boundaries due to variations in the number of words in each column
E Koci [110]	Encoding of spatial interrelations between these regions using a graph representation, as well as rules and heuristics	1) Recognition for single-table and multi-table spreadsheets. 2) No reliance on any assumptions with what regards the arrangement of tables	Tables with few columns and empty cells are not handled well.
SA Siddiqui [51]	deformable CNN + Faster R-CNN	1) The use of deformable convolution can handle various tabular structures. 2) released a new dataset that contained table structure data.	The tables in the proposed approach won't operate correctly if they have a row and column span.
SA Siddiqui [112]	Fully CNNs	The complexity of the task of identifying table structures is reduced by the proposed prediction tiling approach.	1) Additional post-processing processes are necessary when rows or columns are excessively fragmented. 2) The technique is based on the tabular structures' consistency assumption.
SR Qasim [115]	Graph NN + CNN	1) This paper also presents a unique, memory-efficient training strategy based on Monte Carlo. 2) The suggested approach makes use of both textual and spatial characteristics.	The publicly accessible table datasets are not used to test the system.
W Xue [119]	Graph NN + weights depending on distance	For the cell relationship network, the class imbalance issue is solved using the distance-based weighting method.	When dealing with sparse tables, the approach is insecure.
C Tensmeyer [120]	Dilated Convolutions + Fully CNN	The technique is effective with both scanned and PDF document images.	The post-processing heuristics determine how the merging portion of the method works.
SA Khan [113]	RNN	The reduced receptive field of CNNs is solved by the bi-directional GRU.	Pre-processing procedures including binarization, noise reduction, and morphological modification are necessary.
P Riba [54]	Graph Neural Networks approach	1) It is not constrained to rigid tabular layouts in terms of single rows, columns or presence of rule lines. 2) The model is language independent	1) The method may have problems when dealing with border conditions. 2) There is a small amount of training data in the RVL-CDIP dataset and F1, Precision and Recall metrics are lower than other methods.
Y Deng [52]	Encoder decoder net	1) In the work that is given, issues with end-to-end table recognition are examined. 2) Made a contribution with yet another sizable dataset in the area of table comprehension.	The other publicly accessible table recognition datasets are not used to assess the suggested baseline technique.
E Koci [111]	Graph model + Application of genetic-based approaches	Requires little to no involvement of domain experts	The accuracy of GE depends on the number of edges. Specifically, we determined that GE achieves an accuracy of only 19% for multi-table graphs
D Prasad [95]	Cascade mask Regionbased CNN High-Resolution Network-based model	Direct regression occurs at cellular boundaries using an end-to-end method.	Tables with/out ruling lines must undergo further post-processing.
S Raja [116]	Mask R-CNN + ResNet-101 based Net	1) An additional alignment loss is suggested for precise cell detection. 2) A trainable top-down for cell identification and bottom-up for structure recognition collection is proposed.	When cells are empty, the strategy is weak.

Table 4: A comparison of the benefits and drawbacks of several deep learning-based table Structure recognition methods (continue Table 3)

Literature	Method	Benefits	Drawbacks
B Xiao [124]	cells' bounding boxes + conditional attention network	Only utilizes visual features without any meta-data	1) Assumes that the coordinates of cells in the table are known. 2) Difficulties with tables without borders
Y Zou [117]	Fully CNNs	1) Using linked component analysis enhances the outcomes. 2) In a table, cells are segmented in addition to the rows and columns.	To provide comparison findings, a small number of post-processing procedures utilizing specific algorithms are necessary.
X Zhong [66]	Dual decoder with attention-based encoding	1) To assess table recognition techniques, the methodology offers a unique evaluation metric called TEDS. 2) released a huge table dataset.	The technique cannot be readily compared to other state-of-the-art techniques.
KA Hashmi [118]	Utilizing an optimization technique for anchors+ Mask R-CNN	Networks of region proposals converge more quickly and effectively thanks to optimized anchoring.	This study relies on the preliminary pre-processing phase of clustering the ground truth to find appropriate anchors.
A Zucker [107]	Character Region Awareness for Text Detection (CRAFT) and Density-Based Spatial Clustering of Applications with Noise (DBSCAN)	A bottom-up method, which emphasizes that the table structure is formed by relative positions of text cells, and not by inherent boundaries	Cannot handle spreading rows or columns well
X Zheng [103]	Method for object detecting generally	An additional innovative cluster-based technique combined with a hierarchical network to detect tabular forms.	Accurately classifying a table is a prerequisite for final cell structure identification.
Z Zhang [108]	A combination of fully convolutional network (FCN)+ RoI-Align + the pretrained BERT model + Gated Recurrent Unit (GRU) decoder	Directly operates on table images with no dependency on meta-information, can process simple and complex tables	Oversegments tables when space between cells is large, doesn't handle merged cells well
M Namysl [109]	Rule-based algorithms + graph-based table interpretation method	1) Approach allows processing images and digital documents. 2) Processing steps can be adapted separately	1) Support the most frequent table formats only. Reliance on the presence of predefined keywords. 2) Prone to the errors propagated from the upstream components of system. 3) Focus on the tables with rulings
A Nassar [68]	End-to-end neural network + CNN Backbone + transformer based layers	1) Handles different languages without being trained on them. 2) Predicts tables structure and bounding boxes for the table content	Work with PDF documents
A Jain [125]	spatial associations + dynamic programming techniques	Recognizing complex table structures having multi-span rows/columns and missing cells	Uses OCR to read words from images Not language agnostic
S Raja [121]	object detection	Better detection of empty cells	Fails for very sparse tables where most of the cells are empty

present. Second, based on the first stage proposals, it predicts the object's class, refines the bounding box, and creates a mask at the pixel level of the object. The backbone structure is related to both phases. The concept of Mask R-CNN is simple: Faster R-CNN outputs a class label and a bounding-box offset for each candidate object; Mask R-CNN adds a third branch that outputs the object mask.

6.3. HRNets

Ke Sun et al, [129, 130] present a novel architecture called High-Resolution Net, which is capable of maintaining high-resolution representations through

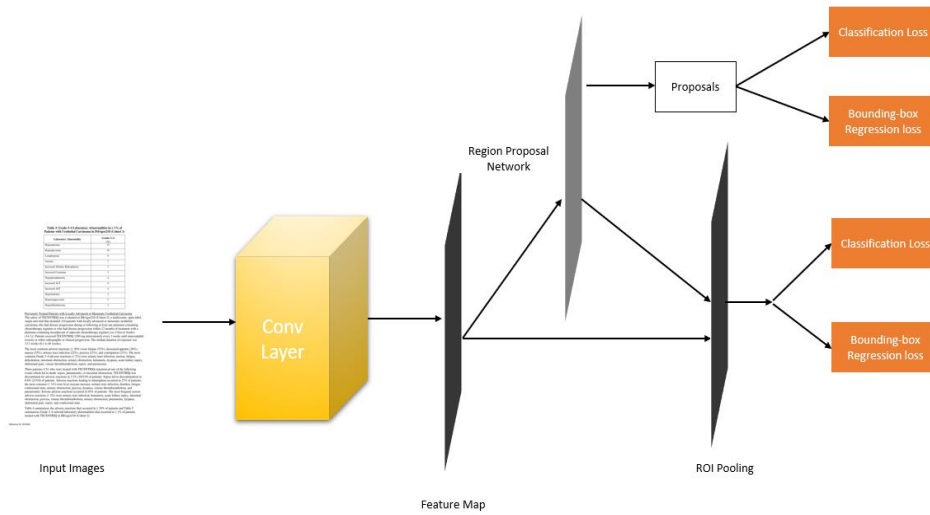


Figure 22: Faster R-CNN

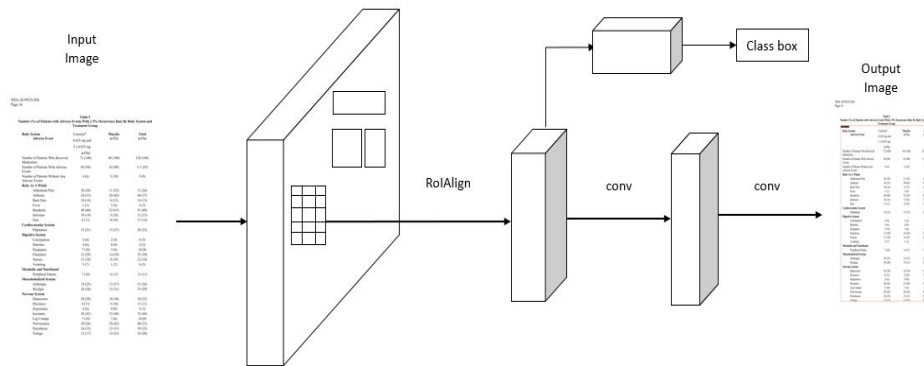


Figure 23: Mask R-CNN

the entire process. The first stage of the HRNet project is to build a high-resolution subnetwork. The next stage is to add more high-to-low resolutions subnetworks. The multi-scale fusions are carried out by HRNet through a parallel multi-resolution network as seen in Fig. 24.

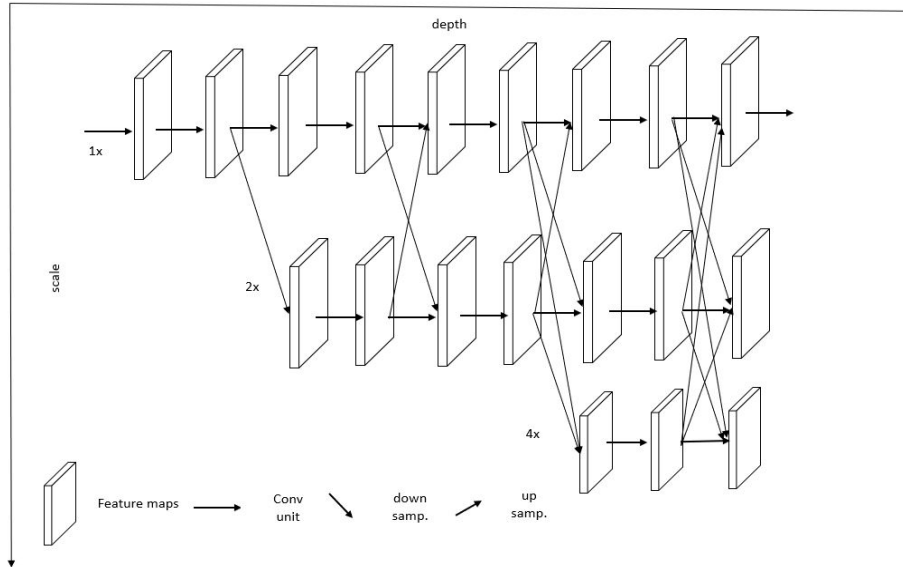


Figure 24: HRNet

Compared to existing widely-used networks [131, 132, 133, 134], HRNet has two advantages: it can connect high-to-low-resolution subnetworks in parallel, and it can provide better pose estimation. Most existing fusion schemes combine low-resolution and high-resolution representations. Instead of doing so, HRNet performs multiscale fusions to boost both the high-resolution and low-resolution representations.

6.4. Resnest

Resnest [135] is a simple architecture that combines the features of a multipath network with a channel-wise attention strategy. It allows for the preservation of independent representations in the meta structure. As in a multi-path network, a Resnet network module performs a set of transformations on low-dimensional embeddings and concatenates their outputs. Each transformation is carried out with a different attention strategy to capture

the interdependencies of a feature map. The key difference between the two is that the attention strategy is focused on the specific channel and not the whole network. The Split-Attention block is a computing unit that combines feature map group and split attention operations. A Split-Attention Block is depicted in Fig. 25.

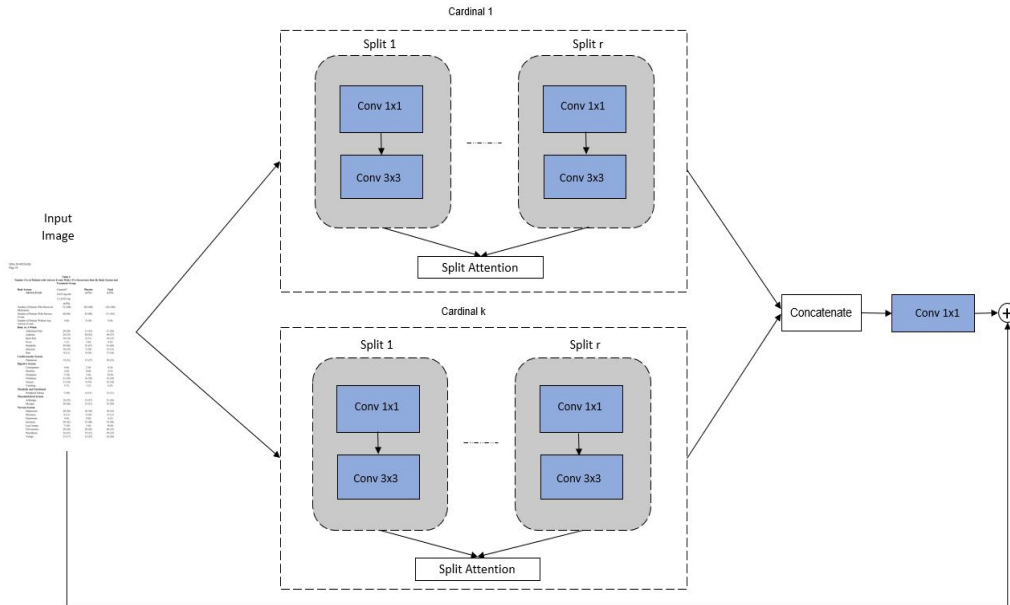


Figure 25: ResneSt

6.5. Dynamic R-CNN

Hongkai Zhang et al, [136] proposes Dynamic RCNN, a simple but effective method for maximizing the dynamic quality of object detection proposals. It is made up of two parts: Dynamic Label Assignment and Dynamic SmoothL1 Loss, which are used for classification and regression, respectively. First, adjust the IoU threshold for positive/negative samples based on the proposals distribution in the training procedure to train a better classifier that is discriminative for high IoU proposals. Set the threshold as the proposal's IoU at a certain percentage because this can reflect the overall distribution's quality. Change the shape of the regression loss function for regression to adaptively fit the regression label distribution change and ensure the contribution of high-quality samples to training.

7. Experiments Results

7.1. Experiment Settings

The MMDetection [137] library for PyTorch has been used to implement each of the proposed and tested models. A vast variety of object detection and instance segmentation methods, as well as associated parts and modules, are included in the object detection toolkit known as MMDetection. It gradually transforms into a single platform that includes several widely used detection techniques and contemporary modules. Three Tesla V100-SXM GPUs with 16 GB of GPU memory, 16 GB of RAM, two Intel Xeon E-5-2680 CPUs, and four NVIDIA Tesla k20x GPUs were used in the trials, which were carried out on the Google Colaboratory platform. With pictures scaled to a constant size of 1300×1500 and a batch size of 16, all models have been trained and evaluated. The optimizer with a momentum of 0.9, a weight decay of 0.0001, and a learning rate of 0.02 is known as SGD. The Feature Pyramid Network (FPN) neck is used by all models.

7.2. Results of TNCR dataset

The Faster R-CNN model has achieved good performance in table detection compared with Cascade-RCNN and Cascade Mask-RCNN in most of the backbones. We have trained the Faster R-CNN model with L1 Loss [138] with Resnet-50 for bounding box regression. As shown in Table 5, it achieves f1-score of 0.921. Resnet-101 backbone achieves the highest F1 score over 50% to 65%, ResNeXt-101-64x4d achieves the highest F1 score over 70% to 95% and ResNeXt-101-64x4d achieves the highest F1 score over 50%:95% of 0.786. Resnet-50 backbone with $1 \times$ Lr schedule achieves the lowest performance over 50% to 60% IoUs. Also, the Resnet-50 backbone with L1 Loss achieves the lowest performance from 65% to 95% IoUs and also achieves the lowest performance over 50%:95%.

We implemented Mask R-CNN [128] to use R-CNN for table objects in an image and also used for performing object segmentation for each ROI. As seen in Table 6, Mask R-CNN shows good performance in our dataset in precision, recall, and F1 score for all backbones. Resnet-101 backbone has achieved the highest F1 score of 0.774 over 50%:95% and maintains the highest F1 score at various IoUs. ResNeXt-101-32x4d achieves the lowest performance over 50% to 95% IoUs and also achieves an f1 score of 0.512 over 50%:95%. ResNeXt-101-64x4d also achieves the lowest performance at various IoUs except for 95% IoU.

Table 5: Faster R-CNN

Backbone	Lr schd/Losses		IoU										
			50%	55%	60%	65%	70%	75%	80%	85%	90%	95%	50%:95%
Resnet-50	LrLoss	Precision	0.875	0.872	0.872	0.866	0.858	0.844	0.823	0.782	0.688	0.424	0.649
		Recall	0.973	0.972	0.970	0.964	0.956	0.941	0.922	0.890	0.812	0.577	0.775
		F1-Score	0.921	0.919	0.918	0.912*	0.904*	0.889*	0.869*	0.832*	0.744*	0.488*	0.706*
Resnet-50	1x	Precision	0.874	0.872	0.871	0.869	0.863	0.844	0.827	0.783	0.693	0.431	0.653
		Recall	0.972	0.969	0.968	0.966	0.959	0.942	0.929	0.895	0.823	0.587	0.779
		F1-Score	0.920*	0.917*	0.916*	0.914	0.908	0.890	0.875	0.835	0.752	0.497	0.710
Resnet-101	1x	Precision	0.885	0.885	0.882	0.879	0.870	0.867	0.849	0.820	0.763	0.555	0.720
		Recall	0.973	0.973	0.971	0.969	0.961	0.956	0.943	0.920	0.870	0.698	0.835
		F1-Score	0.926	0.926	0.924	0.921	0.913	0.909	0.893	0.867	0.812	0.618	0.773
ResNeXt-101-32x4d	1x	Precision	0.880	0.879	0.877	0.875	0.872	0.866	0.845	0.817	0.760	0.575	0.727
		Recall	0.976	0.976	0.975	0.972	0.969	0.962	0.944	0.921	0.871	0.711	0.843
		F1-Score	0.925	0.924	0.923	0.920	0.917	0.911	0.891	0.865	0.811	0.635	0.780
ResNeXt-101-64x4d	1x	Precision	0.884	0.884	0.880	0.879	0.876	0.871	0.856	0.833	0.780	0.581	0.733
		Recall	0.972	0.970	0.969	0.967	0.965	0.961	0.950	0.931	0.884	0.724	0.848
		F1-Score	0.925	0.925	0.922	0.920	0.918	0.913	0.900	0.879	0.828	0.644	0.786

Table 6: Mask R-CNN

Backbone	Lr schd		IoU										
			50%	55%	60%	65%	70%	75%	80%	85%	90%	95%	50%:95%
Resnet-50	1x	Precision	0.877	0.876	0.874	0.871	0.868	0.858	0.834	0.800	0.728	0.506	0.692
		Recall	0.973	0.972	0.970	0.967	0.963	0.952	0.932	0.903	0.840	0.651	0.812
		F1-Score	0.922	0.921	0.919	0.916	0.913	0.902	0.880	0.848	0.779	0.569	0.747
Resnet-101	1x	Precision	0.878	0.877	0.875	0.874	0.869	0.861	0.847	0.812	0.762	0.553	0.716
		Recall	0.977	0.976	0.974	0.973	0.966	0.959	0.949	0.918	0.874	0.711	0.844
		F1-Score	0.924	0.923	0.921	0.920	0.914	0.907	0.895	0.861	0.814	0.622	0.774
ResNeXt-101-32x4d	1x	Precision	0.778	0.777	0.774	0.769	0.759	0.749	0.713	0.651	0.477	0.407	0.434
		Recall	0.975	0.974	0.968	0.964	0.952	0.941	0.913	0.856	0.725	0.695	0.626
		F1-Score	0.865*	0.864*	0.860*	0.855*	0.844*	0.834*	0.800*	0.739*	0.575*	0.513*	0.512*
ResNeXt-101-64x4d	1x	Precision	0.778	0.777	0.774	0.769	0.759	0.749	0.713	0.651	0.477	0.417	0.434
		Recall	0.975	0.974	0.968	0.964	0.952	0.941	0.913	0.856	0.725	0.705	0.626
		F1-Score	0.865	0.864	0.860	0.855	0.844	0.834	0.800	0.739	0.575	0.524	0.512

In the following tables 7 to 12 show the comparative analysis we have trained HRNets with different methods and each method with different backbones for object detection and instance segmentation models. In Table 7, we evaluated and calculated f1-score. It shows that HRNetV2p-W40 achieves better performance over 50% to 65%. Also, HRNetV2p-W18 achieves better performance over 70%, 75%, 80%, and 95%. HRNetV2p-W18 achieves an f1 score of 0.842 over 50%:95% IoU. HRNetV2p-W32 backbone achieves the lowest performance over 50% to 70%, and 90% IoUs and HRNetV2p-W40 achieve the lowest performance over 75% to 85% and 95%. HRNetV2p-W40 achieves f1 score of 0.841 over 50%:95% IoU.

Table 8 shows the performance of the HRNets Faster R-CNN detector with various backbone structures with combinations of Lr Schedule. The HRNetV2p-W18 with 1x Lr Schedule backbone shows a low performance

Table 7: HRNets - Cascade R-CNN

Backbone	Lr schd		IoU										
			50%	55%	60%	65%	70%	75%	80%	85%	90%	95%	50%:95%
HRNetV2p-W18	20e	Precision	0.894	0.894	0.894	0.892	0.892	0.886	0.880	0.862	0.825	0.712	0.803
		Recall	0.962	0.962	0.960	0.960	0.960	0.954	0.950	0.937	0.906	0.813	0.887
		F1-Score	0.926	0.926	0.925	0.924	0.924	0.918	0.913	0.897	0.863	0.759	0.842
HRNetV2p-W32	20e	Precision	0.895	0.895	0.893	0.893	0.893	0.889	0.881	0.869	0.828	0.717	0.806
		Recall	0.955	0.955	0.954	0.954	0.953	0.949	0.943	0.933	0.900	0.810	0.882
		F1-Score	0.924*	0.924*	0.922*	0.922*	0.922*	0.918	0.910	0.899	0.862*	0.760	0.842
HRNetV2p-W40	20e	Precision	0.893	0.891	0.891	0.891	0.888	0.880	0.871	0.854	0.831	0.705	0.799
		Recall	0.967	0.965	0.965	0.964	0.961	0.956	0.948	0.935	0.914	0.811	0.889
		F1-Score	0.928	0.926	0.926	0.926	0.923	0.916*	0.907*	0.892*	0.870	0.754*	0.841*

compared with other backbones. it achieves an f1 score of 0.770. It achieves 3.2% less than HRNetV2p-W18 with 2x Lr Schedule. HRNetV2p-W40 with 1x Lr Schedule backbone achieves better performance over 50% to 85% IoUs and HRNetV2p-W40 with 2x Lr Schedule backbone achieves better performance over 90% and 95% IoUs. HRNetV2p-W18 with 2x Lr Schedule backbone achieves an f1 score of 0.802 over 50%:95%. HRNetV2p-W32 with 1x Lr Schedule backbone share same performance over 50% to 60%.

Table 8: HRNets - Faster R-CNN

Backbone	Lr schd		IoU										
			50%	55%	60%	65%	70%	75%	80%	85%	90%	95%	50%:95%
HRNetV2p-W18	1x	Precision	0.867	0.865	0.863	0.859	0.853	0.845	0.827	0.806	0.750	0.556	0.711
		Recall	0.972	0.970	0.968	0.964	0.959	0.952	0.940	0.915	0.869	0.711	0.842
		F1-Score	0.916*	0.914*	0.912*	0.908*	0.902*	0.895*	0.879*	0.857*	0.805*	0.624*	0.770*
HRNetV2p-W18	2x	Precision	0.876	0.873	0.872	0.869	0.867	0.857	0.845	0.817	0.776	0.628	0.752
		Recall	0.962	0.960	0.958	0.955	0.953	0.946	0.937	0.910	0.874	0.759	0.860
		F1-Score	0.916	0.914	0.912	0.909	0.907	0.899	0.888	0.860	0.822	0.687	0.802
HRNetV2p-W32	1x	Precision	0.877	0.876	0.874	0.869	0.862	0.859	0.839	0.822	0.759	0.579	0.728
		Recall	0.969	0.968	0.967	0.963	0.957	0.954	0.939	0.922	0.870	0.728	0.849
		F1-Score	0.920	0.919	0.918	0.913	0.907	0.904	0.886	0.869	0.810	0.645	0.783
HRNetV2p-W32	2x	Precision	0.877	0.877	0.877	0.874	0.869	0.864	0.847	0.820	0.785	0.592	0.735
		Recall	0.964	0.964	0.963	0.960	0.956	0.951	0.939	0.918	0.886	0.734	0.849
		F1-Score	0.918	0.918	0.917	0.914	0.910	0.905	0.890	0.866	0.832	0.655	0.787
HRNetV2p-W40	1x	Precision	0.875	0.874	0.873	0.872	0.868	0.862	0.851	0.827	0.779	0.612	0.743
		Recall	0.970	0.969	0.968	0.967	0.964	0.958	0.949	0.930	0.888	0.753	0.862
		F1-Score	0.920	0.919	0.918	0.917	0.913	0.907	0.897	0.875	0.829	0.675	0.798
HRNetV2p-W40	2x	Precision	0.880	0.880	0.877	0.877	0.873	0.861	0.852	0.834	0.802	0.629	0.754
		Recall	0.957	0.957	0.954	0.954	0.951	0.943	0.935	0.918	0.890	0.755	0.856
		F1-Score	0.916	0.916	0.913	0.913	0.910	0.900	0.891	0.873	0.843	0.686	0.801

Table 9 shows the performance of the HRNets HTC method with the same Lr Schedule. HRNetV2p-W40 backbone suffers from overfitting through the dataset. HRNetV2p-W18 achieves f1 score of 0.840, precision of 0.901 and recall 0.788 over 50%:95%. HRNetV2p-W18 achieves better performance over various IoUs. HRNetV2p-W32 shows less performance compare with

HRNetV2p-W18 with 8.3% over 50%:95% for the f1 score.

Table 9: HRNets - HTC

Backbone	Lr schd		IoU										
			50%	55%	60%	65%	70%	75%	80%	85%	90%	95%	50%:95%
HRNetV2p-W18	20e	Precision	0.885	0.885	0.883	0.882	0.881	0.875	0.862	0.849	0.808	0.691	0.788
		Recall	0.987	0.987	0.984	0.984	0.982	0.976	0.966	0.954	0.915	0.816	0.901
		F1-Score	0.933	0.933	0.930	0.930	0.928	0.922	0.911	0.898	0.858	0.748	0.840
HRNetV2p-W32	20e	Precision	0.851	0.851	0.849	0.846	0.843	0.834	0.816	0.792	0.737	0.516	0.684
		Recall	0.985	0.985	0.984	0.981	0.976	0.968	0.951	0.929	0.885	0.710	0.848
		F1-Score	0.913*	0.913*	0.911*	0.908*	0.904*	0.896*	0.878*	0.855*	0.804*	0.597*	0.757*

Table 10 shows the performance of HRNets HTC method with the same Lr Schedule. HRNetV2p-W32 has achieved the highest f1 score of 0.871 over 50%:95% and continues to achieve the highest F1 score at various IoUs. HRNetV2p-W32 shows good performance compare with HRNetV2p-W18 with 12% over 50%:95% for f1 score. HRNetV2p-W40 with 1× and 2× Lr Schedule backbones suffer from overfitting through the dataset. Table 11 shows the performance of HRNets Cascade Mask R-CNN method. HRNetV2p-W32 and HRNetV2p-W40 backbones suffer from overfitting through the dataset. HRNetV2p-W18 achieve f1 score of 0.903 over 50%:95%.

Table 10: HRNets - Mask R-CNN

Backbone	Lr schd		IoU										
			50%	55%	60%	65%	70%	75%	80%	85%	90%	95%	50%:95%
HRNetV2p-W18	1x	Precision	0.848	0.845	0.840	0.839	0.835	0.829	0.817	0.793	0.736	0.521	0.684
		Recall	0.971	0.969	0.966	0.964	0.960	0.956	0.947	0.928	0.876	0.698	0.834
		F1-Score	0.905*	0.902*	0.898*	0.897*	0.893*	0.887*	0.877*	0.855*	0.799*	0.596*	0.751*
HRNetV2p-W32	1x	Precision	0.859	0.857	0.857	0.857	0.852	0.848	0.833	0.816	0.764	0.585	0.816
		Recall	0.971	0.969	0.969	0.969	0.965	0.960	0.947	0.934	0.889	0.744	0.934
		F1-Score	0.911	0.909	0.909	0.909	0.904	0.900	0.886	0.871	0.821	0.654	0.871

Table 11: HRNets - Cascade Mask R-CNN

Backbone	Lr schd		IoU										
			50%	55%	60%	65%	70%	75%	80%	85%	90%	95%	50%:95%
HRNetV2p-W18	20e	Precision	0.888	0.887	0.887	0.886	0.885	0.884	0.872	0.858	0.828	0.732	0.810
		Recall	0.970	0.970	0.970	0.967	0.967	0.965	0.955	0.942	0.918	0.836	0.903
		F1-Score	0.927	0.926	0.926	0.924	0.924	0.922	0.911	0.898	0.870	0.780	0.903

Table 12 shows the performance of HRNets with Fully Convolutional One-Stage (FCOS) Object Detection. HRNets FCOS achieves less performance

compared with other models. HRNetV2p-W18 with $2\times$ Lr Schedule achieve an increment of 25% f1 score from HRNetV2p-W18 with $1\times$ Lr Schedule and HRNetV2p-W18 with $2\times$ Lr Schedule achieve an increment of 22.5% f1 score from HRNetV2p-W32. HRNetV2p-W18 with $2\times$ Lr Schedule achieve an f1 score of 0.648.

Table 12: HRNets - FCOS

Backbone	Lr schd		IoU										
			50%	55%	60%	65%	70%	75%	80%	85%	90%	95%	50%:95%
HRNetV2p-W18	1x	Precision	0.511	0.507	0.498	0.485	0.467	0.441	0.405	0.328	0.222	0.086	0.298
		Recall	0.959	0.946	0.930	0.910	0.885	0.844	0.798	0.697	0.517	0.244	0.601
		F1-Score	0.666*	0.660*	0.648*	0.632*	0.611*	0.579*	0.537*	0.446*	0.310*	0.127*	0.398*
HRNetV2p-W18	2x	Precision	0.790	0.788	0.782	0.779	0.770	0.759	0.729	0.691	0.596	0.335	0.563
		Recall	0.983	0.978	0.972	0.969	0.959	0.947	0.917	0.878	0.786	0.545	0.764
		F1-Score	0.875	0.872	0.866	0.863	0.854	0.842	0.812	0.773	0.677	0.414	0.648
HRNetV2p-W32	1x	Precision	0.566	0.561	0.555	0.539	0.528	0.504	0.469	0.400	0.275	0.086	0.326
		Recall	0.970	0.964	0.956	0.928	0.906	0.868	0.818	0.730	0.571	0.241	0.605
		F1-Score	0.714	0.709	0.702	0.681	0.667	0.637	0.596	0.516	0.371	0.126	0.423

In the following tables 13 and 14 show the comparative analysis, we have trained ResNeSt with Cascade R-CNN and Faster R-CNN methods, and each method with different backbones(Resnest-50, Resnest-101). For Cascade R-CNN S-101 backbone achieve an f1 score of 0.845 over 50%:95% IoU and also achieves the highest performance compare with the S-50 backbone and the Faster R-CNN method. The Faster R-CNN S-101 backbone achieves an f1 score of 0.748 over 50%:95% IoU. Cascade R-CNN S-101 backbone has an increment of 9.2% over 50%:95% for the f1 score.

Dynamic RCNN proposes by [136], it is a simple but effective method for maximizing the dynamic quality of object detection proposals. Table 15 show the Dynamic RCNN with Resnet-50 achieves an f1 score of 0.628, the precision of 0.561, recall of 0.714 over 50%:95%.

Table 13: Resnest - Cascade R-CNN

Backbone	Lr schd		IoU										
			50%	55%	60%	65%	70%	75%	80%	85%	90%	95%	50%:95%
S-50	1x	Precision	0.895	0.894	0.891	0.885	0.881	0.875	0.870	0.854	0.808	0.659	0.777
		Recall	0.977	0.976	0.974	0.969	0.965	0.959	0.954	0.940	0.903	0.784	0.880
		F1-Score	0.934	0.933	0.930	0.925	0.921	0.915	0.910	0.894	0.852	0.716	0.825
S-101	1x	Precision	0.905	0.903	0.902	0.899	0.893	0.891	0.884	0.876	0.826	0.693	0.799
		Recall	0.985	0.984	0.983	0.979	0.976	0.972	0.965	0.958	0.917	0.811	0.898
		F1-Score	0.943	0.941	0.940	0.937	0.932	0.929	0.922	0.915	0.869	0.747	0.845

Table 14: Resnest - Faster R-CNN

Backbone	Lr schd		IoU										
			50%	55%	60%	65%	70%	75%	80%	85%	90%	95%	50%:95%
S-50	1x	Precision	0.884	0.884	0.880	0.879	0.872	0.861	0.844	0.809	0.709	0.429	0.656
		Recall	0.970	0.970	0.968	0.967	0.961	0.951	0.935	0.906	0.824	0.597	0.784
		F1-Score	0.925	0.925	0.921	0.920	0.914	0.903	0.887	0.854	0.762	0.499	0.714
S-101	1x	Precision	0.893	0.893	0.890	0.888	0.879	0.876	0.862	0.823	0.747	0.495	0.694
		Recall	0.981	0.979	0.977	0.975	0.967	0.963	0.950	0.921	0.861	0.645	0.813
		F1-Score	0.934	0.934	0.931	0.929	0.920	0.917	0.903	0.869	0.799	0.560	0.748

Table 15: Dynamic R-CNN

Backbone	Lr schd		IoU										
			50%	55%	60%	65%	70%	75%	80%	85%	90%	95%	50%:95%
Resnet-50	1x	Precision	0.855	0.854	0.853	0.849	0.839	0.823	0.802	0.764	0.646	0.267	0.561
		Recall	0.978	0.977	0.975	0.971	0.963	0.943	0.925	0.888	0.793	0.451	0.714
		F1-Score	0.912	0.911	0.909	0.905	0.896	0.878	0.859	0.821	0.711	0.335	0.628

7.3. Result of different datasets

7.3.1. Table Detection Evaluations

To identify the tabular region in the document image and regress the coordinates of a bounding box that has been designated as a tabular region is the task of table detection. Tables 16,17 demonstrates how several table detection techniques that have been thoroughly researched compare in terms of performance. The ICDAR-2013, ICDAR-2017-POD, ICDAR-2019, and UNLV datasets are typically used to assess the effectiveness of table detection algorithms.

Additionally described in Tables 16,17 is the Intersection Over Union (IOU) criterion used to determine precision and recall. The most accurate results across all relevant datasets are underlined. It is important to note that several of the approaches did not specify the IOU threshold value but instead compared their findings to those of other approaches that did. So, for those procedures, we have taken into consideration the same threshold value.

7.3.2. Table Recognition Evaluations

Table recognition entails both segmenting the structure of tables (the task of structural segmentation is assessed based on how precisely the rows or columns of the tables are split) and extracting the data from the cells. We

Table 16: Table detection

Approach	Dataset	Method		IoU											Year		
				50%	55%	60%	65%	70%	75%	80%	85%	90%	95%	50%:95%			
Tesseract [88]	UNLV	Tab-stop Detection	Precision	-	-	-	-	-	-	-	-	-	-	86.00	-	-	2010
			Recall	-	-	-	-	-	-	-	-	-	-	79.00	-	-	
			F1-Score	-	-	-	-	-	-	-	-	-	-	82.35	-	-	
A Gilani[22]	UNLV	Faster R-CNN	Precision	-	-	-	-	-	-	-	-	-	82.30	-	-	2017	
			Recall	-	-	-	-	-	-	-	-	-	90.67	-	-		
			F1-Score	-	-	-	-	-	-	-	-	-	86.29	-	-		
SA Siddiqui[98]	UNLV	Deformable CNN + Faster R-CNN	Precision	78.6	-	-	-	-	-	-	-	-	-	-	-	2018	
			Recall	74.9	-	-	-	-	-	-	-	-	-	-	-		
			F1-Score	76.7	-	-	-	-	-	-	-	-	-	-	-		
Á Casado-García[102]	UNLV	YOLO	Precision	-	-	93.0	-	92.0	-	83.0	-	48.0	-	-	2020		
			Recall	-	-	95.0	-	94.0	-	85.0	-	49.0	-	-			
			F1-Score	-	-	94.0	-	93.0	-	84.0	-	49.0	-	-			
M Agarwal [92]	UNLV	Cascade mask R-CNN	Precision	96.0	-	94.4	-	91.5	-	82.6	-	61.8	-	-	2018		
			Recall	77.0	-	75.8	-	73.4	-	66.3	-	49.6	-	-			
			F1-Score	86.5	-	85.1	-	82.5	-	74.4	-	55.7	-	-			
S Schreiber[20]	ICDAR2013	Mask R-CNN	Precision	97.40	-	-	-	-	-	-	-	-	-	-	2017		
			Recall	96.15	-	-	-	-	-	-	-	-	-	-			
			F1-Score	96.77	-	-	-	-	-	-	-	-	-	-			
SA Siddiqui[51]	ICDAR2013	Deformable CNN	Precision	99.6	-	-	-	-	-	-	-	-	-	-	2018		
			Recall	99.6	-	-	-	-	-	-	-	-	-	-			
			F1-Score	99.6	-	-	-	-	-	-	-	-	-	-			
I Kavasidis[100]	ICDAR2013	Semantic Image Segmentation	Precision	97.5	-	-	-	-	-	-	-	-	-	-	2019		
			Recall	98.1	-	-	-	-	-	-	-	-	-	-			
			F1-Score	97.8	-	-	-	-	-	-	-	-	-	-			
Y Huang[97]	ICDAR2013	YOLO	Precision	100	-	98.6	-	-	-	89.2	-	-	-	-	2019		
			Recall	94.9	-	93.6	-	-	-	84.6	-	-	-	-			
			F1-Score	97.3	-	96.1	-	-	-	86.8	-	-	-	-			
SS Paliwal[96]	ICDAR2013	fully convolutions	Precision	96.97	-	-	-	-	-	-	-	-	-	-	2019		
			Recall	96.28	-	-	-	-	-	-	-	-	-	-			
			F1-Score	96.62	-	-	-	-	-	-	-	-	-	-			
Á Casado-García[102]	ICDAR2013	Mask R-CNN	Precision	-	-	70.0	-	70.0	-	70.0	-	47.0	-	-	2020		
			Recall	-	-	97.0	-	97.0	-	97.0	-	65.0	-	-			
			F1-Score	-	-	81.0	-	81.0	-	81.0	-	54.0	-	-			
D Prasad[95]	ICDAR2013	Cascade mask R-CNN HRNet	Precision	100	-	-	-	-	-	-	-	-	-	-	2020		
			Recall	100	-	-	-	-	-	-	-	-	-	-			
			F1-Score	100	-	-	-	-	-	-	-	-	-	-			
M Li[61]	ICDAR2013	Faster R-CNN	Precision	96.58	-	-	-	-	-	-	-	-	-	-	2020		
			Recall	95.94	-	-	-	-	-	-	-	-	-	-			
			F1-Score	96.25	-	-	-	-	-	-	-	-	-	-			
M Agarwal [92]	ICDAR2013	Cascade mask R-CNN	Precision	100.0	-	100.0	-	98.7	-	94.2	-	66.0	-	-	2021		
			Recall	100.0	-	100.0	-	98.7	-	94.2	-	66.0	-	-			
			F1-Score	100.0	-	100.0	-	98.7	-	94.2	-	66.0	-	-			
X Zheng[103]	ICDAR2013	object detection networks	Precision	98.97	-	-	-	-	-	-	-	-	-	-	2021		
			Recall	99.77	-	-	-	-	-	-	-	-	-	-			
			F1-Score	99.31	-	-	-	-	-	-	-	-	-	-			
SA Siddiqui[51]	ICDAR2017	Deformable CNN	Precision	-	-	96.5	-	-	-	96.7	-	-	-	-	2018		
			Recall	-	-	97.1	-	-	-	93.7	-	-	-	-			
			F1-Score	-	-	96.8	-	-	-	95.2	-	-	-	-			
Y Huang[97]	ICDAR2017	YOLO	Precision	-	-	97.8	-	-	-	97.5	-	-	-	-	2019		
			Recall	-	-	97.2	-	-	-	96.8	-	-	-	-			
			F1-Score	-	-	97.5	-	-	-	97.1	-	-	-	-			

will review the evaluations of the few previously discussed approaches in this part.

Table 18 provides a summary of the findings. It is important to note that the different datasets and evaluation measures used in these procedures mean that the provided methodologies are not directly comparable to one another.

Table 17: Table detection (Continue Table 16)

Approach	Dataset	Method		IoU											Year	
				50%	55%	60%	65%	70%	75%	80%	85%	90%	95%	50%:95%		
Y Li[104]	ICDAR2017	Generative Adversarial Networks(GAN)	Precision	-	-	94.4	-	-	-	90.3	-	-	-	-	-	2019
			Recall	-	-	94.4	-	-	-	90.3	-	-	-	-	-	
			F1-Score	-	-	94.4	-	-	-	90.3	-	-	-	-	-	
N Sun [99]	ICDAR2017	Faster R-CNN	Precision	-	-	-	-	-	94.3	-	-	-	-	-	2019	
			Recall	-	-	-	-	-	95.6	-	-	-	-	-		
			F1-Score	-	-	-	-	-	94.9	-	-	-	-	-		
Á Casado-García[102]	ICDAR2017	RetinaNet	Precision	-	-	92.0	-	92.0	-	89.0	-	79.0	-	-	2020	
			Recall	-	-	87.0	-	87.0	-	84.0	-	75.0	-	-		
			F1-Score	-	-	89.0	-	89.0	-	86.0	-	77.0	-	-		
M Agarwal [92]	ICDAR2017	Cascade mask R-CNN	Precision	-	-	96.9	-	-	-	-	-	-	-	-	2021	
			Recall	-	-	89.9	-	-	-	-	-	-	-	-		
			F1-Score	-	-	93.4	-	-	-	-	-	-	-	-		
D Prasad[95]	ICDAR2019	Cascade mask R-CNN HRNet	Precision	-	-	-	-	-	-	-	-	-	-	-	2020	
			Recall	-	-	-	-	-	-	-	-	-	-	-		
			F1-Score	-	-	94.3	-	93.4	-	92.5	-	90.1	-	-		
M Agarwal [92]	ICDAR2019	Cascade mask R-CNN	Precision	98.7	-	98.0	-	97.7	-	97.1	-	93.4	-	-	2021	
			Recall	94.6	-	93.9	-	93.6	-	93.0	-	89.5	-	-		
			F1-Score	96.6	-	95.9	-	95.6	-	95.0	-	91.5	-	-		
X Zheng[103]	ICDAR2019	object detection networks	Precision	-	-	-	-	-	96.0	-	90.0	-	-	2021		
			Recall	-	-	-	-	-	95.0	-	89.0	-	-			
			F1-Score	-	-	-	-	-	95.5	-	95.5	-	-			
SA Siddiqui[98]	Mormot	Deformable CNN	Precision	84.9	-	-	-	-	-	-	-	-	-	-	2018	
			Recall	94.6	-	-	-	-	-	-	-	-	-	-		
			F1-Score	89.5	-	-	-	-	-	-	-	-	-	-		
M Agarwal [92]	TableBank	Cascade mask R-CNN	Precision	93.4	-	99.5	-	-	-	-	-	-	-	-	2021	
			Recall	92.4	-	97.8	-	-	-	-	-	-	-	-		
			F1-Score	92.9	-	98.6	-	-	-	-	-	-	-	-		
P Riba [54]	RVL-CDIP	Graph NN	Precision	15.2	-	-	-	-	-	-	-	-	-	-	2019	
			Recall	36.5	-	-	-	-	-	-	-	-	-	-		
			F1-Score	21.5	-	-	-	-	-	-	-	-	-	-		

7.4. Open source code

Several open source frameworks for creating generic deep learning models, most of which are written in Python, are available online, including TensorFlow, Keras, PyTorch, and MXNet. The open-source projects for table detection and structure recognition are summarized in Table 19. Many of the authors have also made open-source implementations of their proposed models available. TensorFlow and PyTorch are the most often utilized frameworks in these open source projects.

8. Conclusion

In the field of document analysis, table analysis is a significant and extensively researched problem. The challenge of interpreting tables has been dramatically transformed and new standards have been set thanks to the use of deep learning ideas.

As we said at the paper’s main contribution’s paragraph at the Introduction section, we have addressed several current processes that have advanced

Table 18: Table Structure Recognition

Approach	Dataset	Method		IoU											Year		
				50%	55%	60%	65%	70%	75%	80%	85%	90%	95%	50%:95%			
S Schreiber[20]	ICDAR2013	Fully CNN	Precision	95.93	-	-	-	-	-	-	-	-	-	-	-	-	2017
			Recall	87.36	-	-	-	-	-	-	-	-	-	-	-	-	
			F1-Score	91.44	-	-	-	-	-	-	-	-	-	-	-	-	
SA Siddiqui[51]	ICDAR2013	Deformable CNN	Precision	93.19	-	-	-	-	-	-	-	-	-	-	-	2019	
			Recall	93.08	-	-	-	-	-	-	-	-	-	-	-		
			F1-Score	92.98	-	-	-	-	-	-	-	-	-	-	-		-
W Xue[119]	ICDAR2013	Graph NN + weights depending on distance	Precision	92.6	-	-	-	-	-	-	-	-	-	-	-	2019	
			Recall	44.7	-	-	-	-	-	-	-	-	-	-	-		
			F1-Score	60.3	-	-	-	-	-	-	-	-	-	-	-		-
SS Paliwal[96]	ICDAR2013	fully CNN	Precision	92.15	-	-	-	-	-	-	-	-	-	-	-	2019	
			Recall	89.87	-	-	-	-	-	-	-	-	-	-	-		
			F1-Score	90.98	-	-	-	-	-	-	-	-	-	-	-		-
SA Khan[113]	ICDAR2013	Bi-directional RNN	Precision	96.92	-	-	-	-	-	-	-	-	-	-	-	2019	
			Recall	90.12	-	-	-	-	-	-	-	-	-	-	-		
			F1-Score	93.39	-	-	-	-	-	-	-	-	-	-	-		-
C Tensmeyer[120]	ICDAR2013	Dilated Convolutions + Fully CNN	Precision	95.8	-	-	-	-	-	-	-	-	-	-	-	2019	
			Recall	94.6	-	-	-	-	-	-	-	-	-	-	-		
			F1-Score	95.2	-	-	-	-	-	-	-	-	-	-	-		-
Z Chi[64]	ICDAR2013	Fully CNN	Precision	88.5	-	-	-	-	-	-	-	-	-	-	-	2019	
			Recall	86.0	-	-	-	-	-	-	-	-	-	-	-		
			F1-Score	87.2	-	-	-	-	-	-	-	-	-	-	-		-
Á Casado-García[102]	ICDAR2013	Mask R-CNN	Precision	-	-	70.0	-	70.0	-	70.0	-	47.0	-	-	-	2020	
			Recall	-	-	97.0	-	97.0	-	97.0	-	65.0	-	-	-		
			F1-Score	-	-	81.0	-	81.0	-	81.0	-	54.0	-	-	-		-
S Raja[116]	ICDAR2013	Object Detection Methods	Precision	92.7	-	-	-	-	-	-	-	-	-	-	-	2020	
			Recall	91.1	-	-	-	-	-	-	-	-	-	-	-		
			F1-Score	91.9	-	-	-	-	-	-	-	-	-	-	-		-
KA Hashmi[118]	ICDAR2013	Object Detection Methods	Precision	95.37	-	-	-	-	-	-	-	-	-	-	-	2021	
			Recall	95.56	-	-	-	-	-	-	-	-	-	-	-		
			F1-Score	95.46	-	-	-	-	-	-	-	-	-	-	-		-
D Prasad[95]	ICDAR2019	Object Detection Methods	Precision	-	-	-	-	-	-	-	-	-	-	-	-	2020	
			Recall	-	-	-	-	-	-	-	-	-	-	-	-		
			F1-Score	-	-	43.8	-	35.4	-	19.0	-	3.6	-	-	-		-
Y Zou[117]	ICDAR2019	Fully CNN	Precision	-	-	18.79	-	-	-	1.71	-	-	-	-	-	2021	
			Recall	-	-	10.07	-	-	-	0.92	-	-	-	-	-		
			F1-Score	-	-	13.11	-	-	-	1.19	-	-	-	-	-		-
X Zheng[103]	ICDAR2019	Object Detection Methods	Precision	-	-	-	-	-	-	-	-	-	-	-	-	2021	
			Recall	-	-	-	-	-	-	-	-	-	-	-	-		
			F1-Score	54.8	-	38.5	-	-	-	-	-	-	-	-	-		-

Table 19: Open source code for most of the studies articles in Table Detection

Article	Model	Year	Framework	Link
Z Chi [64]	SciTSR	2019	Pytorch	https://github.com/Academic-Hammer/SciTSR
D Prasad [95]	CascadeTabNet	2020	Pytorch	https://github.com/DevashishPrasad/CascadeTabNet
Á Casado-García [102]	-	2020	mxnet	https://github.com/holms-ur/fine-tuning
M Li [95]	TableBank	2020	Pytorch, Detectron2	https://github.com/doc-analysis/TableBank
S Raja S Raja [116]	TabStructNet	2020	tensorflow	https://github.com/sachinraja13/TabStructNet.git
X Zhong [66]	PubTabNet	2020	-	https://github.com/ibm-aur-nlp/PubTabNet
M Agarwal [92]	CDeC-Net	2021	PyTorch	https://github.com/mdv3101/CDeCNet

the process of information extraction from tables in document pictures by implementing deep learning concepts. We have discussed methods that use deep learning to detect, identify, and classify tables. We have also shown the most and least well-known techniques that have been used to detect and identify tables, respectively.

As we did at section 7, all of the datasets that are publicly accessible and their access details have been compiled. On numerous datasets, we have presented a thorough performance comparison of the methodologies that have been addressed. On well-known datasets that are freely accessible to the public, state-of-the-art algorithms for table detection have produced results that are almost flawless. Once the tabular region has been identified, the work of structurally segmenting tables and then recognizing them follows.

We conclude that both of these areas still have opportunities for development.

References

- [1] J. Hu, R. S. Kashi, D. Lopresti, G. T. Wilfong, Evaluating the performance of table processing algorithms, *International Journal on Document Analysis and Recognition* 4 (3) (2002) 140–153.
- [2] P. Dollár, R. Appel, S. Belongie, P. Perona, Fast feature pyramids for object detection, *IEEE transactions on pattern analysis and machine intelligence* 36 (8) (2014) 1532–1545.
- [3] J. Yang, G. Yang, Modified convolutional neural network based on dropout and the stochastic gradient descent optimizer, *Algorithms* 11 (3) (2018) 28.
- [4] S. Li, W. Liu, G. Xiao, Detection of screw nut images based on deep transfer learning network, in: *2019 Chinese Automation Congress (CAC)*, IEEE, 2019, pp. 951–955.
- [5] K. L. Masita, A. N. Hasan, S. Paul, Pedestrian detection using r-cnn object detector, in: *2018 IEEE Latin American Conference on Computational Intelligence (LA-CCI)*, IEEE, 2018, pp. 1–6.
- [6] Z. Hu, J. Tang, Z. Wang, K. Zhang, L. Zhang, Q. Sun, Deep learning for image-based cancer detection and diagnosis- a survey, *Pattern Recognition* 83 (2018) 134–149.
- [7] J. Redmon, S. Divvala, R. Girshick, A. Farhadi, You only look once: Unified, real-time object detection, in: *Proceedings of the IEEE conference on computer vision and pattern recognition*, 2016, pp. 779–788.

- [8] A. Abdallah, A. Berendeyev, I. Nuradin, D. Nurseitov, Tncr:table net detection and classification dataset, *Neurocomputing* 473 (2022) 79–97. doi:10.1016/j.neucom.2021.11.101.
URL <https://www.sciencedirect.com/science/article/pii/S0925231221018142>
- [9] R. Fakoor, F. Ladhak, A. Nazi, M. Huber, Using deep learning to enhance cancer diagnosis and classification, in: *Proceedings of the international conference on machine learning*, Vol. 28, ACM, New York, USA, 2013, pp. 3937–3949.
- [10] S. Minaee, Z. Liu, Automatic question-answering using a deep similarity neural network, in: *2017 IEEE Global Conference on Signal and Information Processing (GlobalSIP)*, IEEE, 2017, pp. 923–927.
- [11] A. Abdallah, M. Kasem, M. A. Hamada, S. Sdeek, Automated question-answer medical model based on deep learning technology, in: *Proceedings of the 6th International Conference on Engineering & MIS 2020*, 2020, pp. 1–8.
- [12] A. Arpteg, B. Brinne, L. Crnkovic-Friis, J. Bosch, Software engineering challenges of deep learning, in: *2018 44th Euromicro Conference on Software Engineering and Advanced Applications (SEAA)*, IEEE, 2018, pp. 50–59.
- [13] M. A. Hamada, A. Abdallah, M. Kasem, M. Abokhalil, Neural network estimation model to optimize timing and schedule of software projects, in: *2021 IEEE International Conference on Smart Information Systems and Technologies (SIST)*, IEEE, 2021, pp. 1–7.
- [14] M. Mahmoud, M. Kasem, A. Abdallah, H. S. Kang, Ae-lstm: Autoencoder with lstm-based intrusion detection in iot, in: *2022 International Telecommunications Conference (ITC-Egypt)*, IEEE, 2022, pp. 1–6.
- [15] W. Xu, J. Jang-Jaccard, A. Singh, Y. Wei, F. Sabrina, Improving performance of autoencoder-based network anomaly detection on nsl-kdd dataset, *IEEE Access* 9 (2021) 140136–140146.
- [16] S. A. Mahmoud, I. Ahmad, W. G. Al-Khatib, M. Alshayeb, M. T. Parvez, V. Märgner, G. A. Fink, Khatt: An open arabic offline handwritten text database, *Pattern Recognition* 47 (3) (2014) 1096–1112.

- [17] D. Nurseitov, K. Bostanbekov, D. Kurmankhojayev, A. Alimova, A. Abdallah, R. Tolegenov, Handwritten kazakh and russian (hkr) database for text recognition, *Multimedia Tools and Applications* 80 (21) (2021) 33075–33097.
- [18] N. Toiganbayeva, M. Kasem, G. Abdimanap, K. Bostanbekov, A. Abdallah, A. Alimova, D. Nurseitov, Kohtd: Kazakh offline handwritten text dataset, *Signal Processing: Image Communication* 108 (2022) 116827.
- [19] A. Fischer, C. Y. Suen, V. Frinken, K. Riesen, H. Bunke, A fast matching algorithm for graph-based handwriting recognition, in: *International Workshop on Graph-Based Representations in Pattern Recognition*, Springer, 2013, pp. 194–203.
- [20] S. Schreiber, S. Agne, I. Wolf, A. Dengel, S. Ahmed, Deepdesrt: Deep learning for detection and structure recognition of tables in document images, in: *2017 14th IAPR international conference on document analysis and recognition (ICDAR)*, Vol. 1, IEEE, 2017, pp. 1162–1167.
- [21] M. Traquair, E. Kara, B. Kantarci, S. Khan, Deep learning for the detection of tabular information from electronic component datasheets, in: *2019 IEEE Symposium on Computers and Communications (ISCC)*, IEEE, 2019, pp. 1–6.
- [22] A. Gilani, S. R. Qasim, I. Malik, F. Shafait, Table detection using deep learning, in: *2017 14th IAPR international conference on document analysis and recognition (ICDAR)*, Vol. 1, IEEE, 2017, pp. 771–776.
- [23] D. N. Tran, T. A. Tran, A. Oh, S. H. Kim, I. S. Na, Table detection from document image using vertical arrangement of text blocks, *International Journal of Contents* 11 (4) (2015) 77–85.
- [24] L. Hao, L. Gao, X. Yi, Z. Tang, A table detection method for pdf documents based on convolutional neural networks, in: *2016 12th IAPR Workshop on Document Analysis Systems (DAS)*, IEEE, 2016, pp. 287–292.
- [25] S. Mao, A. Rosenfeld, T. Kanungo, Document structure analysis algorithms: a literature survey, *Document recognition and retrieval X* 5010 (2003) 197–207.

- [26] E. Kara, M. Traquair, M. Simsek, B. Kantarci, S. Khan, Holistic design for deep learning-based discovery of tabular structures in datasheet images, *Engineering Applications of Artificial Intelligence* 90 (2020) 103551.
- [27] M. Sarkar, M. Aggarwal, A. Jain, H. Gupta, B. Krishnamurthy, Document structure extraction using prior based high resolution hierarchical semantic segmentation, in: *European Conference on Computer Vision*, Springer, 2020, pp. 649–666.
- [28] R. Zanibbi, D. Blostein, J. R. Cordy, A survey of table recognition, *Document Analysis and Recognition* 7 (1) (2004) 1–16.
- [29] D. W. Embley, M. Hurst, D. Lopresti, G. Nagy, Table-processing paradigms: a research survey, *International Journal of Document Analysis and Recognition (IJDAR)* 8 (2) (2006) 66–86.
- [30] B. Couiasnon, A. Lemaitre, *Recognition of tables and forms* (2014).
- [31] S. Khusro, A. Latif, I. Ullah, On methods and tools of table detection, extraction and annotation in pdf documents, *Journal of Information Science* 41 (1) (2015) 41–57.
- [32] R. Szeliski, *Computer vision: algorithms and applications*, Springer Science & Business Media, 2010.
- [33] B. C. G. Lee, Line detection in binary document scans: a case study with the international tracing service archives, in: *2017 IEEE International Conference on Big Data (Big Data)*, IEEE, 2017, pp. 2256–2261.
- [34] L. Liu, W. Ouyang, X. Wang, P. Fieguth, J. Chen, X. Liu, M. Pietikäinen, Deep learning for generic object detection: A survey, *International journal of computer vision* 128 (2) (2020) 261–318.
- [35] Y. Bengio, A. Courville, P. Vincent, Representation learning: A review and new perspectives, *IEEE transactions on pattern analysis and machine intelligence* 35 (8) (2013) 1798–1828.
- [36] Y. LeCun, Y. Bengio, G. Hinton, et al., Deep learning. *nature*, 521 (7553), 436–444, Google Scholar Google Scholar Cross Ref Cross Ref (2015).

- [37] I. Goodfellow, Y. Bengio, A. Courville, Deep learning, MIT press, 2016.
- [38] G. Litjens, T. Kooi, B. E. Bejnordi, A. A. A. Setio, F. Ciompi, M. Ghafoorian, J. A. Van Der Laak, B. Van Ginneken, C. I. Sánchez, A survey on deep learning in medical image analysis, *Medical image analysis* 42 (2017) 60–88.
- [39] X. X. Zhu, D. Tuia, L. Mou, G.-S. Xia, L. Zhang, F. Xu, F. Fraundorfer, Deep learning in remote sensing: A comprehensive review and list of resources, *IEEE Geoscience and Remote Sensing Magazine* 5 (4) (2017) 8–36.
- [40] J. Gu, Z. Wang, J. Kuen, L. Ma, A. Shahroudy, B. Shuai, T. Liu, X. Wang, G. Wang, J. Cai, et al., Recent advances in convolutional neural networks, *Pattern Recognition* 77 (2018) 354–377.
- [41] S. Pouyanfar, S. Sadiq, Y. Yan, H. Tian, Y. Tao, M. P. Reyes, M.-L. Shyu, S.-C. Chen, S. S. Iyengar, A survey on deep learning: Algorithms, techniques, and applications, *ACM Computing Surveys (CSUR)* 51 (5) (2018) 1–36.
- [42] T. Young, D. Hazarika, S. Poria, E. Cambria, Recent trends in deep learning based natural language processing, *IEEE Computational Intelligence Magazine* 13 (3) (2018) 55–75.
- [43] J. Zhou, G. Cui, S. Hu, Z. Zhang, C. Yang, Z. Liu, L. Wang, C. Li, M. Sun, Graph neural networks: A review of methods and applications, *AI Open* 1 (2020) 57–81.
- [44] Z. Zhang, J. Geiger, J. Pohjalainen, A. E.-D. Mousa, W. Jin, B. Schuller, Deep learning for environmentally robust speech recognition: An overview of recent developments, *ACM Transactions on Intelligent Systems and Technology (TIST)* 9 (5) (2018) 1–28.
- [45] Z. Wu, S. Pan, F. Chen, G. Long, C. Zhang, S. Y. Philip, A comprehensive survey on graph neural networks, *IEEE transactions on neural networks and learning systems* 32 (1) (2020) 4–24.
- [46] M. D. Zeiler, R. Fergus, Visualizing and understanding convolutional networks, in: *European conference on computer vision*, Springer, 2014, pp. 818–833.

- [47] M. Oquab, L. Bottou, I. Laptev, J. Sivic, Learning and transferring mid-level image representations using convolutional neural networks, in: Proceedings of the IEEE conference on computer vision and pattern recognition, 2014, pp. 1717–1724.
- [48] M. Göbel, T. Hassan, E. Oro, G. Orsi, Icdar 2013 table competition, in: 2013 12th International Conference on Document Analysis and Recognition, IEEE, 2013, pp. 1449–1453.
- [49] L. Gao, X. Yi, Z. Jiang, L. Hao, Z. Tang, Icdar2017 competition on page object detection, in: 2017 14th IAPR International Conference on Document Analysis and Recognition (ICDAR), Vol. 1, IEEE, 2017, pp. 1417–1422.
- [50] L. Gao, Y. Huang, H. Déjean, J.-L. Meunier, Q. Yan, Y. Fang, F. Kleber, E. Lang, Icdar 2019 competition on table detection and recognition (ctdar), in: 2019 International Conference on Document Analysis and Recognition (ICDAR), IEEE, 2019, pp. 1510–1515.
- [51] S. A. Siddiqui, I. A. Fateh, S. T. R. Rizvi, A. Dengel, S. Ahmed, Deeptabstr: deep learning based table structure recognition, in: 2019 International Conference on Document Analysis and Recognition (ICDAR), IEEE, 2019, pp. 1403–1409.
- [52] Y. Deng, D. Rosenberg, G. Mann, Challenges in end-to-end neural scientific table recognition, in: 2019 International Conference on Document Analysis and Recognition (ICDAR), IEEE, 2019, pp. 894–901.
- [53] A. W. Harley, A. Ufkes, K. G. Derpanis, Evaluation of deep convolutional nets for document image classification and retrieval, in: 2015 13th International Conference on Document Analysis and Recognition (ICDAR), IEEE, 2015, pp. 991–995.
- [54] P. Riba, A. Dutta, L. Goldmann, A. Fornés, O. Ramos, J. Lladós, Table detection in invoice documents by graph neural networks, in: 2019 International Conference on Document Analysis and Recognition (ICDAR), IEEE, 2019, pp. 122–127.
- [55] A. Mondal, P. Lipps, C. Jawahar, Iiit-ar-13k: a new dataset for graphical object detection in documents, in: International Workshop on Document Analysis Systems, Springer, 2020, pp. 216–230.

- [56] W. Seo, H. I. Koo, N. I. Cho, Junction-based table detection in camera-captured document images, *International Journal on Document Analysis and Recognition (IJDAR)* 18 (1) (2015) 47–57.
- [57] A. Shahab, F. Shafait, T. Kieninger, A. Dengel, An open approach towards the benchmarking of table structure recognition systems, in: *Proceedings of the 9th IAPR International Workshop on Document Analysis Systems*, 2010, pp. 113–120.
- [58] I. T. Phillips, User’s reference manual for the uw english/technical document image database iii, *UW-III English/technical document image database manual* (1996).
- [59] J. Hu, R. Kashi, D. Lopresti, G. Nagy, G. Wilfong, Why table ground-truthing is hard, in: *Proceedings of Sixth International Conference on Document Analysis and Recognition*, IEEE, 2001, pp. 129–133.
- [60] J. Fang, X. Tao, Z. Tang, R. Qiu, Y. Liu, Dataset, ground-truth and performance metrics for table detection evaluation, in: *2012 10th IAPR International Workshop on Document Analysis Systems*, IEEE, 2012, pp. 445–449.
- [61] M. Li, L. Cui, S. Huang, F. Wei, M. Zhou, Z. Li, Tablebank: Table benchmark for image-based table detection and recognition, in: *Proceedings of the 12th Language Resources and Evaluation Conference*, 2020, pp. 1918–1925.
- [62] N. Siegel, N. Lourie, R. Power, W. Ammar, Extracting scientific figures with distantly supervised neural networks, in: *Proceedings of the 18th ACM/IEEE on joint conference on digital libraries*, 2018, pp. 223–232.
- [63] B. Smock, R. Pesala, R. Abraham, W. Redmond, Pubtables-1m: Towards comprehensive table extraction from unstructured documents, *arXiv preprint arXiv:2110.00061* (2021).
- [64] Z. Chi, H. Huang, H.-D. Xu, H. Yu, W. Yin, X.-L. Mao, Complicated table structure recognition, *arXiv preprint arXiv:1908.04729* (2019).
- [65] X. Zheng, D. Burdick, L. Popa, P. Zhong, N. X. R. Wang, Global table extractor (gte): A framework for joint table identification and

cell structure recognition using visual context, Winter Conference for Applications in Computer Vision (WACV) (2021).

- [66] X. Zhong, E. ShafieiBavani, A. Jimeno Yepes, Image-based table recognition: data, model, and evaluation, in: European Conference on Computer Vision, Springer, 2020, pp. 564–580.
- [67] A. Abdallah, A. Berendeyev, I. Nuradin, D. Nurseitov, Tncr: Table net detection and classification dataset, *Neurocomputing* 473 (2022) 79–97.
- [68] A. Nassar, N. Livathinos, M. Lysak, P. Staar, Tableformer: Table structure understanding with transformers, in: Proceedings of the IEEE/CVF Conference on Computer Vision and Pattern Recognition, 2022, pp. 4614–4623.
- [69] P. Pyreddy, W. Croft, Tinti: A system for retrieval in text tables title2 (1997).
- [70] Y. Wangt, I. T. Phillipst, R. Haralick, Automatic table ground truth generation and a background-analysis-based table structure extraction method, in: Proceedings of Sixth International Conference on Document Analysis and Recognition, IEEE, 2001, pp. 528–532.
- [71] M. A. Jahan, R. G. Ragel, Locating tables in scanned documents for reconstructing and republishing, in: 7th International Conference on Information and Automation for Sustainability, IEEE, 2014, pp. 1–6.
- [72] K. Itonori, Table structure recognition based on textblock arrangement and ruled line position, in: Proceedings of 2nd International Conference on Document Analysis and Recognition (ICDAR'93), IEEE, 1993, pp. 765–768.
- [73] S. Chandran, R. Kasturi, Structural recognition of tabulated data, in: Proceedings of 2nd International Conference on Document Analysis and Recognition (ICDAR'93), IEEE, 1993, pp. 516–519.
- [74] T. Hassan, R. Baumgartner, Table recognition and understanding from pdf files, in: Ninth International Conference on Document Analysis and Recognition (ICDAR 2007), Vol. 2, IEEE, 2007, pp. 1143–1147.

- [75] E. Oro, M. Ruffolo, Trex: An approach for recognizing and extracting tables from pdf documents, in: 2009 10th International Conference on Document Analysis and Recognition, IEEE, 2009, pp. 906–910.
- [76] A. Nurminen, Algorithmic extraction of data in tables in pdf documents, Master’s thesis (2013).
- [77] J. Fang, P. Mitra, Z. Tang, C. L. Giles, Table header detection and classification, in: Twenty-Sixth AAAI Conference on Artificial Intelligence, 2012.
- [78] G. Harit, A. Bansal, Table detection in document images using header and trailer patterns, in: Proceedings of the Eighth Indian Conference on Computer Vision, Graphics and Image Processing, 2012, pp. 1–8.
- [79] S. Tupaj, Z. Shi, C. H. Chang, H. Alam, Extracting tabular information from text files, EECS Department, Tufts University, Medford, USA 1 (1996).
- [80] T. Kieninger, A. Dengel, The t-recs table recognition and analysis system, in: International Workshop on Document Analysis Systems, Springer, 1998, pp. 255–270.
- [81] F. Cesarini, S. Marinai, L. Sarti, G. Soda, Trainable table location in document images, in: Object recognition supported by user interaction for service robots, Vol. 3, IEEE, 2002, pp. 236–240.
- [82] M. Fan, D. S. Kim, Table region detection on large-scale pdf files without labeled data, CoRR, abs/1506.08891 (2015).
- [83] Y. Wang, J. Hu, A machine learning based approach for table detection on the web, in: Proceedings of the 11th international conference on World Wide Web, 2002, pp. 242–250.
- [84] T. Kasar, P. Barlas, S. Adam, C. Chatelain, T. Paquet, Learning to detect tables in scanned document images using line information, in: 2013 12th International Conference on Document Analysis and Recognition, IEEE, 2013, pp. 1185–1189.
- [85] A. C. e Silva, Learning rich hidden markov models in document analysis: Table location, in: 2009 10th International Conference on Document Analysis and Recognition, IEEE, 2009, pp. 843–847.

- [86] S. Klampfl, K. Jack, R. Kern, A comparison of two unsupervised table recognition methods from digital scientific articles, *D-Lib Magazine* 20 (11) (2014) 7.
- [87] L. O’Gorman, The document spectrum for page layout analysis, *IEEE Transactions on pattern analysis and machine intelligence* 15 (11) (1993) 1162–1173.
- [88] F. Shafait, R. Smith, Table detection in heterogeneous documents, in: *Proceedings of the 9th IAPR International Workshop on Document Analysis Systems*, 2010, pp. 65–72.
- [89] D. He, S. Cohen, B. Price, D. Kifer, C. L. Giles, Multi-scale multi-task fcn for semantic page segmentation and table detection, in: *2017 14th IAPR International Conference on Document Analysis and Recognition (ICDAR)*, Vol. 1, IEEE, 2017, pp. 254–261.
- [90] S. Arif, F. Shafait, Table detection in document images using foreground and background features, in: *2018 Digital Image Computing: Techniques and Applications (DICTA)*, IEEE, 2018, pp. 1–8.
- [91] M. M. Reza, S. S. Bukhari, M. Jenckel, A. Dengel, Table localization and segmentation using gan and cnn, in: *2019 International Conference on Document Analysis and Recognition Workshops (ICDARW)*, Vol. 5, IEEE, 2019, pp. 152–157.
- [92] M. Agarwal, A. Mondal, C. Jawahar, Cdec-net: Composite deformable cascade network for table detection in document images, in: *2020 25th International Conference on Pattern Recognition (ICPR)*, IEEE, 2021, pp. 9491–9498.
- [93] N. Carion, F. Massa, G. Synnaeve, N. Usunier, A. Kirillov, S. Zagoruyko, End-to-end object detection with transformers, in: *European conference on computer vision*, Springer, 2020, pp. 213–229.
- [94] J. Li, Y. Xu, T. Lv, L. Cui, C. Zhang, F. Wei, Dit: Self-supervised pre-training for document image transformer, *arXiv preprint arXiv:2203.02378* (2022).

- [95] D. Prasad, A. Gadpal, K. Kapadni, M. Visave, K. Sultanpure, Cascadetabnet: An approach for end to end table detection and structure recognition from image-based documents, in: Proceedings of the IEEE/CVF conference on computer vision and pattern recognition workshops, 2020, pp. 572–573.
- [96] S. S. Paliwal, D. Vishwanath, R. Rahul, M. Sharma, L. Vig, Tablenet: Deep learning model for end-to-end table detection and tabular data extraction from scanned document images, in: 2019 International Conference on Document Analysis and Recognition (ICDAR), IEEE, 2019, pp. 128–133.
- [97] Y. Huang, Q. Yan, Y. Li, Y. Chen, X. Wang, L. Gao, Z. Tang, A yolo-based table detection method, in: 2019 International Conference on Document Analysis and Recognition (ICDAR), IEEE, 2019, pp. 813–818.
- [98] S. A. Siddiqui, M. I. Malik, S. Agne, A. Dengel, S. Ahmed, Decnt: Deep deformable cnn for table detection, IEEE access 6 (2018) 74151–74161.
- [99] N. Sun, Y. Zhu, X. Hu, Faster r-cnn based table detection combining corner locating, in: 2019 International Conference on Document Analysis and Recognition (ICDAR), IEEE, 2019, pp. 1314–1319.
- [100] I. Kavasidis, C. Pino, S. Palazzo, F. Rundo, D. Giordano, P. Messina, C. Spampinato, A saliency-based convolutional neural network for table and chart detection in digitized documents, in: International conference on image analysis and processing, Springer, 2019, pp. 292–302.
- [101] M. Holeček, A. Hoskovec, P. Baudiš, P. Klinger, Table understanding in structured documents, in: 2019 International Conference on Document Analysis and Recognition Workshops (ICDARW), Vol. 5, IEEE, 2019, pp. 158–164.
- [102] Á. Casado-García, C. Domínguez, J. Heras, E. Mata, V. Pascual, The benefits of close-domain fine-tuning for table detection in document images, in: International workshop on document analysis systems, Springer, 2020, pp. 199–215.
- [103] X. Zheng, D. Burdick, L. Popa, X. Zhong, N. X. R. Wang, Global table extractor (gte): A framework for joint table identification and

- cell structure recognition using visual context, in: Proceedings of the IEEE/CVF winter conference on applications of computer vision, 2021, pp. 697–706.
- [104] Y. Li, L. Gao, Z. Tang, Q. Yan, Y. Huang, A gan-based feature generator for table detection, in: 2019 International Conference on Document Analysis and Recognition (ICDAR), IEEE, 2019, pp. 763–768.
 - [105] D.-D. Nguyen, Tablesegnet: a fully convolutional network for table detection and segmentation in document images, *International Journal on Document Analysis and Recognition (IJDAR)* 25 (1) (2022) 1–14.
 - [106] D. Zhang, R. Mao, R. Guo, Y. Jiang, J. Zhu, Yolo-table: disclosure document table detection with involution, *International Journal on Document Analysis and Recognition (IJDAR)* (2022) 1–14.
 - [107] A. Zucker, Y. Belkada, H. Vu, V. N. Nguyen, Clusti: Clustering method for table structure recognition in scanned images, *Mobile Networks and Applications* 26 (4) (2021) 1765–1776.
 - [108] Z. Zhang, J. Zhang, J. Du, F. Wang, Split, embed and merge: An accurate table structure recognizer, *Pattern Recognition* 126 (2022) 108565.
 - [109] M. Namysl, A. M. Esser, S. Behnke, J. Köhler, Flexible table recognition and semantic interpretation system., in: VISIGRAPP (4: VISAPP), 2022, pp. 27–37.
 - [110] E. Koci, M. Thiele, W. Lehner, O. Romero, Table recognition in spreadsheets via a graph representation, in: 2018 13th IAPR International Workshop on Document Analysis Systems (DAS), IEEE, 2018, pp. 139–144.
 - [111] E. Koci, M. Thiele, O. Romero, W. Lehner, A genetic-based search for adaptive table recognition in spreadsheets, in: 2019 International Conference on Document Analysis and Recognition (ICDAR), IEEE, 2019, pp. 1274–1279.
 - [112] S. A. Siddiqui, P. I. Khan, A. Dengel, S. Ahmed, Rethinking semantic segmentation for table structure recognition in documents, in: 2019

International Conference on Document Analysis and Recognition (ICDAR), IEEE, 2019, pp. 1397–1402.

- [113] S. A. Khan, S. M. D. Khalid, M. A. Shahzad, F. Shafait, Table structure extraction with bi-directional gated recurrent unit networks, in: 2019 International Conference on Document Analysis and Recognition (ICDAR), IEEE, 2019, pp. 1366–1371.
- [114] S. F. Rashid, A. Akmal, M. Adnan, A. A. Aslam, A. Dengel, Table recognition in heterogeneous documents using machine learning, in: 2017 14th IAPR International conference on document analysis and recognition (ICDAR), Vol. 1, IEEE, 2017, pp. 777–782.
- [115] S. R. Qasim, H. Mahmood, F. Shafait, Rethinking table recognition using graph neural networks, in: 2019 International Conference on Document Analysis and Recognition (ICDAR), IEEE, 2019, pp. 142–147.
- [116] S. Raja, A. Mondal, C. Jawahar, Table structure recognition using top-down and bottom-up cues, in: European Conference on Computer Vision, Springer, 2020, pp. 70–86.
- [117] Y. Zou, J. Ma, A deep semantic segmentation model for image-based table structure recognition, in: 2020 15th IEEE International Conference on Signal Processing (ICSP), Vol. 1, IEEE, 2020, pp. 274–280.
- [118] K. A. Hashmi, D. Stricker, M. Liwicki, M. N. Afzal, M. Z. Afzal, Guided table structure recognition through anchor optimization, IEEE Access 9 (2021) 113521–113534.
- [119] W. Xue, Q. Li, D. Tao, Res2tim: Reconstruct syntactic structures from table images, in: 2019 International Conference on Document Analysis and Recognition (ICDAR), IEEE, 2019, pp. 749–755.
- [120] C. Tensmeyer, V. I. Morariu, B. Price, S. Cohen, T. Martinez, Deep splitting and merging for table structure decomposition, in: 2019 International Conference on Document Analysis and Recognition (ICDAR), IEEE, 2019, pp. 114–121.
- [121] S. Raja, A. Mondal, C. Jawahar, Visual understanding of complex table structures from document images, in: Proceedings of the IEEE/CVF

Winter Conference on Applications of Computer Vision, 2022, pp. 2299–2308.

- [122] X. Shen, L. Kong, Y. Bao, Y. Zhou, W. Liu, Rcanet: A rows and columns aggregated network for table structure recognition, in: 2022 3rd Information Communication Technologies Conference (ICTC), IEEE, 2022, pp. 112–116.
- [123] C. Ma, W. Lin, L. Sun, Q. Huo, Robust table detection and structure recognition from heterogeneous document images, arXiv preprint arXiv:2203.09056 (2022).
- [124] B. Xiao, M. Simsek, B. Kantarci, A. A. Alkheir, Table structure recognition with conditional attention, arXiv preprint arXiv:2203.03819 (2022).
- [125] A. Jain, S. Paliwal, M. Sharma, L. Vig, Tsr-dsaw: Table structure recognition via deep spatial association of words, arXiv preprint arXiv:2203.06873 (2022).
- [126] H. Li, L. Zeng, W. Zhang, J. Zhang, J. Fan, M. Zhang, A two-phase approach for recognizing tables with complex structures, in: International Conference on Database Systems for Advanced Applications, Springer, 2022, pp. 587–595.
- [127] S. Ren, K. He, R. Girshick, J. Sun, Faster r-cnn: Towards real-time object detection with region proposal networks, arXiv preprint arXiv:1506.01497 (2015).
- [128] K. He, G. Gkioxari, P. Dollar, R. Girshick, Mask r-cnn, 2017 IEEE International Conference on Computer Vision (ICCV) (Oct 2017).
- [129] K. Sun, B. Xiao, D. Liu, J. Wang, Deep high-resolution representation learning for human pose estimation, in: CVPR, 2019.
- [130] K. Sun, Y. Zhao, B. Jiang, T. Cheng, B. Xiao, D. Liu, Y. Mu, X. Wang, W. Liu, J. Wang, High-resolution representations for labeling pixels and regions, CoRR abs/1904.04514 (2019).
- [131] A. Newell, K. Yang, J. Deng, Stacked hourglass networks for human pose estimation, in: European conference on computer vision, Springer, 2016, pp. 483–499.

- [132] E. Insafutdinov, L. Pishchulin, B. Andres, M. Andriluka, B. Schiele, Deepcut: A deeper, stronger, and faster multi-person pose estimation model, in: European Conference on Computer Vision, Springer, 2016, pp. 34–50.
- [133] B. Xiao, H. Wu, Y. Wei, Simple baselines for human pose estimation and tracking, in: Proceedings of the European conference on computer vision (ECCV), 2018, pp. 466–481.
- [134] W. Yang, S. Li, W. Ouyang, H. Li, X. Wang, Learning feature pyramids for human pose estimation, in: proceedings of the IEEE international conference on computer vision, 2017, pp. 1281–1290.
- [135] H. Zhang, C. Wu, Z. Zhang, Y. Zhu, Z. Zhang, H. Lin, Y. Sun, T. He, J. Muller, R. Manmatha, M. Li, A. Smola, Resnest: Split-attention networks, arXiv preprint arXiv:2004.08955 (2020).
- [136] H. Zhang, H. Chang, B. Ma, N. Wang, X. Chen, Dynamic R-CNN: Towards high quality object detection via dynamic training, arXiv preprint arXiv:2004.06002 (2020).
- [137] K. Chen, J. Wang, J. Pang, Y. Cao, Y. Xiong, X. Li, S. Sun, W. Feng, Z. Liu, J. Xu, et al., Mmdetection: Open mmlab detection toolbox and benchmark, arXiv preprint arXiv:1906.07155 (2019).
- [138] S. Wu, J. Yang, X. Wang, X. Li, Iou-balanced loss functions for single-stage object detection, arXiv preprint arXiv:1908.05641 (2019).